



**Assessment of Hematite Nanoparticles as Adsorbent for Arsenic  
Removal**

by

Mahbuboor Rahman Choudhury

**MASTER OF SCIENCE IN CIVIL ENGINEERING (ENVIRONMENTAL)**

Department of Civil Engineering

BANGLADESH UNIVERSITY OF ENGINEERING AND TECHNOLOGY

2009



**Assessment of Hematite Nanoparticles as Adsorbent for Arsenic  
Removal**

by

Mahbuboor Rahman Choudhury

A thesis submitted to the Department of Civil Engineering of Bangladesh University  
of Engineering and Technology, Dhaka, in partial fulfilment of the requirements for  
the degree of

**MASTER OF SCIENCE IN CIVIL ENGINEERING (ENVIRONMENTAL)**

2009

The thesis titled “**Assessment of Hematite Nanoparticles as Adsorbent for Arsenic Removal**” submitted by Mahbuboor Rahman Choudhury, Student No. 100604153(P), and Session: October 2006 has been accepted as satisfactory in partial fulfilment of the requirement for the degree of M.Sc. Engineering (Civil and Environmental) on 24<sup>th</sup> January, 2009.

#### BOARD OF EXAMINERS



---

**Dr. M. Ashraf Ali**  
Professor  
Department of Civil Engineering, BUET, Dhaka

**Chairman**  
(Supervisor)



---

**Dr. Md. Delwar Hossain**  
Professor  
Department of Civil Engineering, BUET, Dhaka

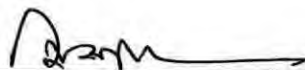
**Member**



---

**Dr. A. B. M. Badruzzaman**  
Professor  
Department of Civil Engineering, BUET, Dhaka

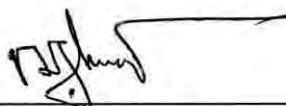
**Member**



---

**Dr. Muhammad Zakaria**  
Professor and Head  
Department of Civil Engineering, BUET, Dhaka

**Member**  
(Ex-officio)



---

**Mr. Md. Serajuddin**  
Superintending Engineer  
DWASA, Karwan Bazar, Dhaka

**Member**  
(External)

## **DECLARATION**

It is hereby declared that this thesis or any part of it has not been submitted elsewhere for the award of any degree or diploma.

24<sup>th</sup> January, 2009



---

**Mahbubor Rahman Choudhury**

**Dedicated**

**To**

**My Family & My Friends**

## TABLE OF CONTENTS

	<b>Page No.</b>
<b>Declaration</b>	iv
<b>Dedication</b>	v
<b>List of Figures</b>	ix
<b>List of Tables</b>	xii
<b>List of Abbreviations</b>	xiii
<b>Acknowledgement</b>	xiv
<b>Abstract</b>	xv
<b>Chapter 1</b>	<b>INTRODUCTION</b>
1.1	Background 1
1.2	Objectives Of The Present Research 3
1.3	Organization Of The Thesis 5
<b>Chapter 2</b>	<b>LITERATURE REVIEW</b>
2.1	Introduction 6
2.2	Historical Review 7
2.3	Occurance Of Arsenic 8
2.4	Arsenic Mobilization In Groundwater 10
2.5	Drinking Water Standards Relating To Arsenic 11
2.6	Health Effects Of Arsenic 11
2.7	Arsenic Contamination Of Groundwater In Bangladesh 12
2.8	Inherent Limitations Of Existing Techniques Used For Arsenic Removal From Water 16
2.8.1	Anion Exchange Resins 16
2.8.2	Activated Alumina / Iron Coated Sand 16
2.8.3	Granular Iron Oxide-based Media 17
2.8.4	Iron Flocculation Process 17
2.8.5	Membrane Techniques 17

	2.9	Surface Area Of Common Adsorbents	18
	2.10	Use Of Iron Nanoparticles For Arsenic Removal	18
	2.11	Evaluation Of Kinetic Rate Constants Of Adsorption	22
	2.12	Summary	23
<b>Chapter</b>	<b>3</b>	<b>CHARACTERIZATION OF THE HEMATITE NANOPARTICLES</b>	
	3.1	Introduction	24
	3.2	Methodology For Physical Characterization Of Hematite Nanoparticles	25
	3.2.1	Potentiometric Titration of Hematite Nanoparticles	25
	3.2.2	X-ray Diffraction (XRD) analysis	26
	3.2.3	BET (Brunauer-Emmett-Teller) surface area analysis	27
	3.2.4	DLS (Dynamic Light Scattering) analysis	27
	3.3	Results And Discussion	29
	3.3.1	Size and Distribution of Hematite Nanoparticles	29
	3.3.2	Specific Surface Area of Hematite Nanoparticles	31
	3.3.3	Structure and Composition of Hematite Nanoparticles	33
	3.3.4	Surface Charge of Hematite Nanoparticles as a function of pH	35
	3.4	Summary	36
<b>Chapter</b>	<b>4</b>	<b>ADSORPTION OF ARSENIC ON HEMATITE NANOPARTICLES</b>	
	4.1	Introduction	38
	4.2	Methodology	39
	4.2.1	Batch Adsorption Experiments	39
	4.2.2	Kinetics of Arsenic adsorption on Hematite Nanoparticles	43
	4.2.3	Laboratory Analysis of Water Samples	44
	4.2.4	Chemicals and Reagents used	45
	4.3	Results And Discussion	45

4.3.1	Effect of pH on Arsenic adsorption	45
4.3.2	Effect of Dispersion of Hematite Nanoparticles	48
4.3.3	Adsorption of Arsenic on Hematite Nanoparticles	49
4.3.4	Adsorption of Phosphate on Hematite Nanoparticles	56
4.3.5	Effect of Phosphate on Adsorption of Arsenic	57
4.3.6	Kinetics of Arsenic Adsorption on Hematite Nanoparticles	58
4.4	Summary	61
<b>Chapter 5</b>	<b>CONCLUSIONS AND RECOMMENDATIONS</b>	
5.1	Conclusions	63
5.2	Recommendations	65
	<b>REFERENCES</b>	67



## List of Figures

		Page No.
Figure 2.1	Alchemical symbol for arsenic	7
Figure 2.2	A large sample of native arsenic	9
Figure 2.3	Realgar	9
Figure 2.4	Distribution of arsenic concentration in Bangladesh based on the nationwide survey carried out by BGS/DPHE	13
Figure 2.5	Distribution of Arsenicosis Patients in Bangladesh (BAMWSP, 2005)	15
Figure 2.6	Nanoscale iron particles for in situ remediation	20
Figure 2.7	Illustration of a permeable reactive barrier remediating a plume	21
Figure 2.8 (a)	Adsorption of Arsenic to 11.72 nm Magnetite at pH 8.0: As(III). (Yean et al., 2005)	22
Figure 2.8 (b)	Adsorption of Arsenic to 11.72 nm Magnetite at pH 8.0: As(V). (Yean et al., 2005)	22
Figure 3.1	TEM image of Hematite Nanoparticles (from website of Nanostructured & Amorphous Materials, Inc.)	25
Figure 3.2	Average hydrodynamic radius of magnetite and hematite nanoparticle aqueous suspensions.	29
Figure 3.3	Aggregation profiles of hematite NPs with and without the biological buffers.	30
Figure 3.4	Aggregation rate constants of magnetite and hematite NPs with and without the biological buffers.	30
Figure 3.5	Adsorption isotherm of N <sub>2</sub> to the iron nanoparticles. The samples were degassed up to $5 \times 10^{-3}$ Torr at 300°C	32
Figure 3.6	Pore size distribution of iron nanoparticles	33
Figure 3.7	XRD pattern of Hematite Nanoparticles	34
Figure 3.8	Surface Charge Density of hematite nanoparticles as a function of pH	35
Figure 3.9	Potentiometric Titration Curves (pH versus TOTM, mM)	36

Figure 4.1	Effect of Sonication on Dispersion of Hematite Nanoparticles	41
Figure 4.2	Equilibration of the Hematite Suspension in an End-over-end Rotator	41
Figure 4.3	Adsorption Envelopes of As(III) and As(V) with Hematite NP at 0.1 M ionic strength (0.133 mol As/ kg Hematite)	47
Figure 4.4 (a)	Langmuir Adsorption Isotherm for As(III) on Hematite Nanoparticles in a 0.1 g/L suspension at pH 5.15	50
Figure 4.4 (b)	Langmuir Adsorption Isotherm for As(III) on Hematite Nanoparticles in a 0.1 g/L suspension at pH 6.1	50
Figure 4.4 (c)	Langmuir Adsorption Isotherm for As(III) on Hematite Nanoparticles in a 0.1 g/L suspension at pH 7.5	50
Figure 4.4 (d)	Freundlich Adsorption Isotherm for As(III) on Hematite Nanoparticles in a 0.1 g/L suspension at pH 5.15	50
Figure 4.4 (e)	Freundlich Adsorption Isotherm for As(III) on Hematite Nanoparticles in a 0.1 g/L suspension at pH 6.1	50
Figure 4.4 (f)	Freundlich Adsorption Isotherm for As(III) on Hematite Nanoparticles in a 0.1 g/L suspension at pH 7.5	50
Figure 4.5 (a)	Langmuir Adsorption Isotherm for As(V) on Hematite Nanoparticles in a 0.1 g/L suspension at pH 5.15	51
Figure 4.5 (b)	Langmuir Adsorption Isotherm for As(V) on Hematite Nanoparticles in a 0.1 g/L suspension at pH 6.1	51
Figure 4.5 (c)	Langmuir Adsorption Isotherm for As(V) on Hematite Nanoparticles in a 0.1 g/L suspension at pH 7.5	51
Figure 4.5 (d)	Freundlich Adsorption Isotherm for As(V) on Hematite Nanoparticles in a 0.1 g/L suspension at pH 5.15	51
Figure 4.5 (e)	Freundlich Adsorption Isotherm for As(V) on Hematite Nanoparticles in a 0.1 g/L suspension at pH 6.1	51
Figure 4.5 (f)	Freundlich Adsorption Isotherm for As(V) on Hematite Nanoparticles in a 0.1 g/L suspension at pH 7.5	51
Figure 4.6 (a)	Adsorption of Arsenic to 11.72 nm Magnetite at pH 8.0: As(III). (Yean et al., 2005)	53
Figure 4.6 (b)	Adsorption of Arsenic to 11.72 nm Magnetite at pH 8.0: As(V). (Yean et al., 2005)	53

Figure 4.7 (a)	Adsorption of Arsenite and Arsenate on HNPs: pH 5.15	54
Figure 4.7 (b)	Plot of the Adsorption of Arsenite and Arsenate on HNPs: pH 6.10	54
Figure 4.8	Effects of Co-existing Phosphate on Arsenite and Arsenate Removal at Fixed Initial Arsenic Concentration (0.5ppm) (pH $6.15 \pm 0.5$ , 0.1 g/L suspension)	57
Figure 4.9	Kinetics of Arsenic [(a) Arsenite, As(III); (b) Arsenate, As(V)] Removal and Change in Concentration of Arsenic Species in the Aqueous Phase with Time. Initial Arsenic = 13.3 mM; Adsorbent content = 0.1 g/L; pH 6.1	59
Figure 4.10	$\log(q_e - q)$ versus $t$ .	60
Figure 4.11	$t/q$ versus $t$ .	60

## List of Tables

		Page No.
Table 2.1	Arsenic compounds and species and their environmental and toxicological importance in water	10
Table 2.2	Toxicological effects due exposure to high arsenic concentration in drinking water (WHO, 1996; Khan, 1997)	11
Table 2.3	Specific Surface Area (SSA) of common adsorbents used for As Removal	18
Table 3.1	Details of commercially procured hematite nanoparticles	25
Table 3.2	Estimated surface area of the iron nanoparticles using BET method	32
Table 4.1	Effect of hematite aggregation on adsorption of arsenite, As(III)	48
Table 4.2	Langmuir and Freundlich isotherm parameters for As(V) and As(III) adsorption on Hematite Nanoparticles	49
Table 4.3	Maximum arsenic adsorption capacities of some adsorbent system	52
Table 4.4	Adsorption of Arsenic from Groundwater on Hematite Nanoparticles (0.1 g/L) at pH 7.5. (Initial Arsenic Concentration = 1.0ppm)	56
Table 4.5	Adsorption results of Phosphate on Hematite Nanoparticles	56
Table 4.6	Comparison of the first-order and second-order adsorption rate constants, and calculated and experimental $q_e$ values for both As(V) and As(III).	61

## List of Abbreviation

AAS	Atomic Absorption Spectrophotometer
BAMWSP	Bangladesh Arsenic Mitigation Water Supply Project
BET	Brunauer-Emmett-Teller
BGS	British Geological Survey
CHES	2-(Cyclohexylamino) Ethane-Sulfonic Acid
DLS	Dynamic Light Scattering
DPHE	Department Of Public Health Engineering
HEPES	2-[4-(2-Hydroxyethyl)-1-Piperazine] Ethanesulfonic Acid
HNP	Hematite Nanoparticle
MES	2-Morpholinoethanesulfonic Acid Monohydrate
NIPSOM	National Institute Of Preventive And Social Medicine
SFCA	Surfactant Free Cellulose Acetate
SSA	Specific Surface Area
TEM	Transmission Electron Microscope
USEPA	United States Environmental Protection Agency
WHO	World Health Organization
XRD	X-Ray Diffraction

## ACKNOWLEDGEMENT

First of all I want to pay my gratitude to my thesis supervisor, Dr. M. Ashraf Ali, for providing me continuous support and guideline to perform this research work and to prepare this concerted dissertation. His contribution to me can only be acknowledged but never be compensated. His consistent inspiration helped me to work diligently throughout the completion of this research work and also contributed to my ability to approach and solve a problem.

I would like to express my deepest gratitude to the Department of Civil Engineering, BUET, The Head of the Department of Civil Engineering and all the members of BPGS committee to give me such a great opportunity of doing my M.Sc. and this contemporary research work on environmental nanotechnology. I would like to render sincere gratitude to Dr. A.B.M. Badruzzaman for providing assistance to this study through MIT-BUET joint research project and also for providing effective guidance and support throughout the course of this thesis work.

I would like to convey my heartiest thanks especially to Dr. Navid Bin Saleh (currently an Assistant Professor at University of South Carolina, USA), who performed the characterization tests (DLS analysis, BET analysis) of the hematite nanoparticles. Dr. Navid Bin Saleh provided me with his valuable time and effort from his busy research schedules to perform the DLS and BET experiments in the laboratory of Yale University, where he worked as a Post-doctoral Research Associate. Also I would like to thank Dr. Manjura Hoque, Atomic Energy Commission, Dhaka, Bangladesh for performing the XRD analysis of the hematite nanoparticles.

Furthermore, I want to thank Mr. Ehsan and Mr. Mithu of Environmental Engineering Laboratory for frequent support in the laboratory work through out the whole thesis work.

I would like to convey my gratefulness and thanks to all my family members, friends and colleagues; especially my wife Trina for her patience, my friends for their encouragements, and my family for their cordial cooperation and help. Their support and coordination during the thesis period was generous and indispensable.

At last I want to thank my department, all the members of the defense board and respected supervisor Dr. M. Ashraf Ali once again for giving me such an opportunity, which has obviously enhanced my knowledge and skills as an environmental engineer to a great extent.

Mahbuboor Rahman Choudhury

## ABSTRACT

Widespread presence of elevated levels of arsenic (As) in groundwater is a major public health concern in Bangladesh. Although a number of methods are presently used for removal of As from groundwater, they all suffer from certain drawbacks. Technologies based on nanoparticles (typically 1-100 nm in size) have received significant attention in recent times regarding their prospective use in groundwater treatment (e.g., for As removal). However, because their minuscule size, nanoparticles cannot be used directly in an As removal system. For developing such a system, it is extremely important to characterize the nanoparticle itself (e.g. size, aggregation characteristics, etc.) and also to assess their adsorption characteristics. In this study, adsorption characteristics of arsenic on commercially procured hematite nanoparticles (HNPs) have been assessed in laboratory batch experiments.

Characterization tests of the commercially procured HNPs were carried out to assess the structure, composition, particle size, distribution, specific surface area and surface charge. The XRD analysis confirmed structure of the  $\alpha$ -Fe<sub>2</sub>O<sub>3</sub> (Hematite) nanoparticles and absence of significant impurity. The specific surface area of the nanoparticles found from the BET test (13.8m<sup>2</sup>/g) was well below the manufactured-reported value of 50m<sup>2</sup>/g. Potentiometric titration revealed the pH of zero surface charge (i.e., pH<sub>PZC</sub>) of HNPs to be around pH 6.5, which is an important parameter in assessing the adsorption characteristics. An important finding of the DLS test was that the hydrodynamic radius (R<sub>h</sub>) of the HNPs in aqueous suspension was over four times the actual size of the particles.

Batch adsorption tests were carried out under different conditions (e.g. varying pH, presence of competing anions) in order to evaluate the suitability of HNPs for use in As removal. Effect of pH on adsorption of both arsenite and arsenate appear to follow the same trend. Adsorption of arsenite was more than that of arsenate for pH>5.0 under similar conditions. For pH<5.0 the adsorption of arsenite and arsenate was almost similar. With increasing pH there was an initial decrease of arsenate adsorption onto hematite nanoparticles with the maximum adsorption of 0.065 mol/kg occurring at around pH 4.0 and minimum adsorption of 0.040 mol/kg at around pH 7.0. As pH increased further, adsorption of arsenate increased gradually to about 0.058 mol/kg at around pH 10.0. Similar but less pronounced trend was observed for the adsorption of arsenite on HNPs. The effect of pH on adsorption of As could be explained by the aggregation characteristics of HNPs and charge on the aqueous arsenic species. Adsorption isotherms showed that the maximum As adsorption capacity (590μmol/g at pH 9.3) was more than that of arsenate (435μmol/g at pH 6.1). However, at lower concentration of As (<17μmol/L), the adsorption of arsenate was more than that of arsenite. Significant reduction in the adsorption of both arsenite and arsenate on HNPs was observed in the presence of co-existing phosphate (PO<sub>4</sub><sup>3-</sup>). Adsorption of As from natural groundwater on the HNPs was also found to be lower than that from aqueous solution containing indifferent electrolyte NaNO<sub>3</sub>. These results suggest significant effect of competing ions and aggregation properties of HNPs on As adsorption. The effect of dispersion of the HNPs on adsorption was found to be significant. Kinetics experiments showed that As adsorption reached equilibrium within 24 hours, with majority of adsorption taking place within the first few hours.

The results of arsenic adsorption on HNPs indicates that along with other adsorbents (e.g., MnO<sub>2</sub>, Goethite, Alumina, Fe(OH)<sub>3</sub>, TiO<sub>2</sub>), the HNPs could be used as an effective adsorbent for As removal. The higher arsenite adsorption capacity of HNPs could potentially be used in removing As from groundwater (without the necessity of an oxidizing agent), where it is present primarily as arsenite. HNPs could be used for both *in-situ* and *ex-situ* treatment of groundwater; however, such treatment systems must be carefully designed keeping in mind the adsorption as well as aggregation characteristics of the nanoparticles.



## INTRODUCTION

### 1.1 Background

In Bangladesh, arsenic was first tested and detected in groundwater samples from the district of Chapai Nawabgonj bordering the West-Bengal district of India in the late 1993. Since then awareness about the presence of arsenic has been growing in Bangladesh. High levels of arsenic have been detected in 268 upazillas (administrative unit) out of 465; with the southern, south-western and north-eastern regions of the country being mostly affected (BGS/DPHE, 2001). Arsenic contamination has primarily affected the shallow aquifers, which are used for both domestic water supply and irrigation purposes. Eight to twelve million wells across the country constitute the backbone of the rural water supply system. Arsenic contamination of ground water has created a major problem among the rural people as it is estimated that about 35 million people in Bangladesh are exposed to an arsenic concentration in drinking water exceeding the national standard of 50ppb and 57 million people exposed to a concentration exceeding the WHO guideline value of 10ppb (BGS/DPHE, 2001).

Arsenic in drinking water, present primarily as inorganic As (III) (arsenite), has been linked to a number of human ailments. Arsenic exposure via drinking water causes a range of diseases which include cancers, dermal lesions and other skin diseases. In oxygen-rich waters, As (V) (arsenate) will be the predominant oxidation state with  $\text{H}_2\text{AsO}_4^-$  and  $\text{HAsO}_4^{2-}$  being the main anions present. Under more reducing conditions, e.g. in groundwater, As (III) species are stable, with un-dissociated  $\text{H}_3\text{AsO}_3$  predominating at pH values less than 8.

There are a number of commercially available arsenic removal methods that are suitable for the treatment of drinking water. These include anion exchange resins,



granular iron oxide-based media, activated alumina, granular zirconia and titania, and iron/alum flocculation processes (Driehaus et al., 1998; Berdal et al., 2000; Rubel, 2003; Badruzzaman and Westerhoff, 2005). Although all of these methods can, in theory, reduce arsenic below the required 50 µg/L level, each suffers from drawbacks. The polymeric anion exchanges have a low selectivity for arsenate, and certain anions such as sulfate, phosphate competes with arsenate for available anion exchange sites resulting in a short operational life. Many of the granular iron oxihydroxide-based, porous media have a very high affinity for arsenate and a negligible affinity for other common anions, such as sulfate, bicarbonate, and chloride (Meng et al., 2000). However, a major drawback, which is causing operational problems, is the low structural stability of many of the granular media (North, 2005). These granular media cannot be regenerated due to their low physical strength. Coagulation using iron floc as a treatment method is highly effective at removing arsenic from water but generates large amounts of a ferric hydroxide floc, which will require safe disposal in a landfill. Capital equipment requirements are generally high, due to difficulties of effectively separating ferric hydroxide floc from solution.

The recent use of iron nanoparticles as sorbent has led to a radical change in the treatment method used for arsenic removal. Nanoscale iron particles represent a new generation of environmental remediation technologies that could provide cost-effective solutions to some of the most challenging environmental cleanup problems. Nanoscale iron particles have large surface areas and high surface reactivity. Equally important, they provide enormous flexibility for *in situ* applications.

In addition to nanoscale zero-valent iron (NZVI), which is a suitable material for both in-situ and ex-situ groundwater treatment, iron oxide nanoparticles are also suitably used for groundwater remediation. Numerous studies demonstrate that iron oxides have a high affinity for the adsorption of arsenite and arsenate. However the sorption behavior of arsenic is strongly influenced by solution pH values and presence of other competing ions (Dixit and Hering, 2003). By appropriately dispersing hydrated iron oxide (HFO) nanoparticles within a polymeric cation or

anion exchanger, its amphoteric sorption capacity can be tailored to remove either metal cations or anionic ligands. Such hybrid cation and anion exchangers are also amenable to efficient regeneration. Thus, toxic metals and ligands can be separated and recovered quantitatively from the same solution using HFO nanosorbent but with different ion exchanger support (Puttamraju and Sengupta, 2006).

The use of magnetite nanoparticles as a sorbent for arsenic uptake has taken the attention of researcher all around the world. The use of hydrous iron oxide nanoparticles coupled with a highly porous polymer substrate forms the basis of ArsenX<sup>np</sup>, a hybrid inorganic/organic sorbent that has been developed for the removal of arsenic from drinking water (Sylvester et al., 2007).

The advent of iron oxide nanoparticles have opened up a new dimension in the water treatment realm. The high surface area available for adsorption of nanoparticles hold great possibility for using it as a filtering material to remove not only arsenic but other common environmental contaminants also.

Hence the study of other iron oxide nanoparticles (like Hematite,  $\alpha\text{-Fe}_2\text{O}_3$ ), for which relatively little information is available in the literature, in terms of their arsenic adsorption capacity will provide increased option for selection of materials in both ex-situ and in-situ treatment of arsenic contaminated water. It is necessary to study the state of the iron oxide nanoparticles dispersed into arsenic contaminated water. The extent of knowledge about the adsorption characteristics of arsenic on iron oxide nanoparticles is very limited. There appears to be a lack of information on the adsorption characteristics of arsenic on hematite nanoparticles.

## 1.2 Objectives Of The Present Research

The objective of the present study is to assess the arsenic adsorption characteristics of hematite nanoparticles under different experimental conditions. Specific objective of this study include:

- (a) Characterization of the hematite nanoparticles.
- (b) Determination of the effect of dispersion of hematite nanoparticles on the adsorption of arsenic.
- (c) Development of adsorption isotherms and adsorption envelopes of arsenic on hematite nanoparticles.
- (d) Assessment of adsorption kinetics of arsenic on hematite nanoparticles.
- (e) Assessment of the effect of selected water quality parameters (pH, phosphate content) on adsorption of arsenic on hematite nanoparticles.
- (f) Assessment of the adsorption mechanism of arsenic on hematite nanoparticles, including effect of surface charge and intrinsic affinity of arsenic.

The intended research work is aimed at achieving knowledge on various issues related to the arsenic adsorption capacity of hematite nanoparticles. The possible outcomes of the proposed study include: (i) Understanding of the composition, particle size, size distribution and surface area of the hematite nanoparticles. (ii) Understanding the aggregation characteristics of hematite nanoparticles and its impact on the adsorption of the arsenic. The hematite nanoparticles, for their minuscule size, cannot be used directly in an arsenic removal system. Common options are either to use nanoparticle-water slurry or to anchor nanomaterials in a solid matrix, which then could be used for arsenic removal. For developing such system, it is extremely important to characterize the nanomaterial itself (e.g. size, aggregation characteristics etc.) and also the adsorption characteristics of nanoparticles. (iii) Estimation of adsorption capacities of the hematite nanoparticles at different pH. (iv) Appreciation of the important water quality parameters affecting adsorption of arsenic on hematite nanoparticles. (v) Understanding of arsenic

adsorption mechanism of hematite nanoparticles. (vi) Assessment of the potential of hematite nanoparticles for development of an effective adsorbent for arsenic removal.

### 1.3 Organization Of The Thesis

Apart from this chapter, the remainder of the thesis has been divided into four chapters. Chapter 2 presents literature review concerning the history, uses and behavior of arsenic in the environment. This chapter briefly reviews the situation of arsenic contamination in Bangladesh, existing methods of arsenic removal from water and their inherent advantages and disadvantages. There is also a short overview of the use of iron nanoparticles for environmental remediation and the past studies on the adsorption characteristics of iron oxide nanoparticles.

Chapter 3 presents the results of laboratory experiments designed for the characterization of the hematite nanoparticles. The characterization tests of the hematite nanoparticles include potentiometric titration, determining size and size distribution using DLS (Dynamic Light Scattering), specific surface area determination using BET (Brunauer-Emmett-Teller), determination of structure and composition of the nanoparticles using X-Ray Diffraction. These characterization tests were carried out to get a better appreciation of the adsorption mechanism of arsenic on hematite nanoparticles.

Chapter 4 presents the results of laboratory experiments intended to assess the adsorption characteristics of arsenic onto hematite nanoparticles and effect of various parameters, e.g., pH, phosphate concentration of water, dispersion of particles and time on the adsorption mechanism. The implications of the results on arsenic accumulation on hematite nanoparticles have also been discussed in this chapter.

Finally, chapter 5 presents the major conclusions of the study and also provides recommendations for future study.

---

## LITERATURE REVIEW

### 2.1 Introduction

Arsenic is a member of the Nitrogen family with both metallic and nonmetallic properties, and the cycling of arsenic in the environment is regulated by natural processes and human activities. It is the twentieth most common element in the Earth's crust. Arsenic occurs in many forms, but is most toxic as an ion because it reacts with sulfur-containing groups on certain enzymes. Exposure to non-lethal levels of arsenic over a long period of time may result in chronic poisoning and carcinogenic effects. For this reason, arsenic remains a work safety issue in industries where it is still used, such as in the manufacture of weed killers and insecticides, the preservation of wood, and in the extraction of lead and copper ores. The symptoms of acute arsenic poisoning occur in two forms. In the paralytic form, a severe paralysis develops within 1-2 hours, often accompanied by signs of delirium. In the gastrointestinal form, symptoms such as nausea, headache, intense pain, vomiting and diarrhea are dominant. It may be introduced into water through the dissolution of minerals and ores. Arsenic is naturally found at concentration levels of about 0.4 to 30 ng/m<sup>3</sup> in the atmospheric air, about 0.4 to 120 µg/kg in food and at concentrations from undetectable level to a few µg/L in natural water. Thus, humans all over the world are exposed to small amounts of arsenic, mostly through food, water and air. Groundwater contamination by this toxic element has been reported from several countries viz. Argentina, Mongolia, China, Taiwan, Thailand, Mexico, Chile, Hungary, Greece, Ghana and some parts of USA, but the extent of groundwater arsenic contamination in Bangladesh is by far the most severe arsenic contamination, both in terms of area and population exposed.

This chapter enfold historical reviews, occurrence, health concerns, and drinking water standards relating to arsenic. Also it briefly summarizes the status of arsenic contamination in groundwater of Bangladesh. This chapter then describes the conventional arsenic removal technologies in practice, along with their inherent limitations and the use of different adsorbents for arsenic removal. It also reviews the potential use of iron oxide nanoparticles for removal of arsenic. Finally a comparison among different adsorbents used for arsenic removal is presented for better evaluation of the present research work.

## 2.2 Historical Review

The word *arsenic* is borrowed from the Persian word *Zarnikh* meaning "yellow orpiment". *Zarnikh* was borrowed by Greek as *arsenikon*, which means masculine or potent. Arsenic has been known and used in Persia and elsewhere since ancient times (Bentley and Chasteen, 2002). As the symptoms of arsenic poisoning were somewhat ill-defined, it was frequently used for murder until the advent of the Marsh test, a sensitive chemical test for its presence. (Another less sensitive but more general test is the Reinsch test.) Due to its use by the ruling class to murder one another and its potency and discreetness, arsenic has been called the *Poison of Kings* and the *King of Poisons*.

During the Bronze Age, arsenic was often included in bronze, which made the alloy harder (so-called "arsenical bronze"). Arsenic was first isolated by Geber (721-815), an Arabian alchemist (George Sarton). Albertus Magnus (Albert the Great, 1193-1280) is believed to have been the first European to isolate the element in 1250 (Emsley, 2001) In 1649, Johann Schröder published two ways of preparing arsenic.

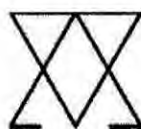


**Figure 2.1 :** Alchemical symbol for arsenic.

(Source: <http://en.wikipedia.org/wiki/Arsenic>)

Cadet's fuming liquid, the first organometallic compound, was synthesized in 1760 by Louis Claude Cadet de Gassicourt by the reaction of potassium acetate with arsenic trioxide (Seyferth, 2001).

In the Victorian era, "arsenic" (colourless, crystalline, soluble "white arsenic") was mixed with vinegar and chalk and eaten by women to improve the complexion of their faces, making their skin paler to show they did not work in the fields. Arsenic was also rubbed into the faces and arms of women to "improve their complexion". The accidental use of arsenic in the adulteration of foodstuffs led to the Bradford sweet poisoning in 1858, which resulted in approximately 20 deaths and 200 people taken ill with arsenic poisoning (Turner, 1999).

Arsenic contamination was first detected in Bangladesh in late 1993 in the district of Chapai Nawabganj in the western Bangladesh. Since then high concentrations of arsenic have been detected in 270 out of 465 upazillas of the country, mostly in the water from the shallow aquifer.

### 2.3 Occurance Of Arsenic

Arsenopyrite, also unofficially called mispickel (King, 2002) ( $\text{FeAsS}$ ) is the most common arsenic-bearing mineral. The most important compounds of arsenic are arsenic (III) oxide,  $\text{As}_2\text{O}_3$ , ("white arsenic"), the yellow sulfide orpiment ( $\text{As}_2\text{S}_3$ ) and red realgar ( $\text{As}_4\text{S}_4$ ) (Figure: 2.3), Paris Green, calcium arsenate, and lead hydrogen arsenate. The latter three have been used as agricultural insecticides and poisons. Orpiment and realgar were formerly used as painting pigments, though they have fallen out of use due to their toxicity and reactivity. Although arsenic is sometimes found native in nature (Figure: 2.2), its main economic source is the mineral arsenopyrite mentioned above; it is also found in arsenides of metals such as silver, cobalt (cobaltite:  $\text{CoAsS}$  and skutterudite:  $\text{CoAs}_3$ ) and nickel, as sulfides, and when oxidised as arsenate minerals such as mimetite,  $\text{Pb}_5(\text{AsO}_4)_3\text{Cl}$  and erythrite,  $\text{Co}_3(\text{AsO}_4)_2 \cdot 8\text{H}_2\text{O}$ , and more rarely arsenites (arsenite(III),  $\text{AsO}_3^{3-}$ ) as opposed to

arsenate (V),  $\text{AsO}_4^{3-}$ ).

In addition to the inorganic forms mentioned above, arsenic also occurs in various organic forms in the environment. Arsenic occurs in water in several different forms, depending upon the pH and the redox potential,  $E_h$ .



**Figure 2.2:** A large sample of native arsenic.

(Source: <http://en.wikipedia.org/wiki/Arsenic>)

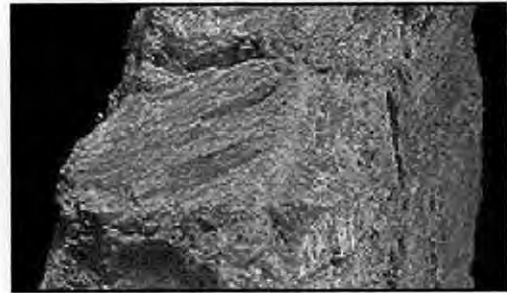


**Figure 2.3:** Realgar

(Source: <http://en.wikipedia.org/wiki/Arsenic>)

Some of the most important compounds and species are shown in table 2.1. In groundwater, arsenic primarily exists as inorganic arsenic. Inorganic trivalent arsenic As(III) or arsenite is the dominant form in reducing environment; while inorganic pentavalent arsenic As(V) or arsenate is the dominant form in oxidizing or aerobic environment. In groundwater environment where the conditions are mostly reducing, a significant part of the arsenic exists as As(III).

As shown in Table 2.1, in the pH range of most groundwater (i.e. pH 6-9), dominant chemical form of As(III) is  $\text{H}_3\text{AsO}_3$ ; while dominant chemical forms of As(V) in this pH range are:  $\text{H}_2\text{AsO}_4^-$ ,  $\text{HAsO}_4^{2-}$ .



<b>Table 2.1:</b> Arsenic compounds and species and their environmental and toxicological importance in water			
<b>Compounds</b>	<b>Example</b>	<b>Environmental Significance/ Dominant pH region</b>	<b>Toxicity</b>
<i>Arsine</i>	As <sup>3-</sup>	Minor Importance	Most Toxic As species
<i>Elemental Arsenic</i>	As	Minor Importance	Least Toxic As species
<i>Trivalent Arsenic</i>	As(III)	Anaerobic	10 times more toxic than As(V)
Arsenite, Inorganic	H <sub>3</sub> AsO <sub>3</sub> , H <sub>2</sub> AsO <sub>3</sub> <sup>1-</sup> , HAsO <sub>3</sub> <sup>2-</sup> , AsO <sub>3</sub> <sup>3-</sup> .	pH = 0-9 pH = 10-12 pH = 13 pH = 14	
Methylated As(III) Organo-As(III)		Minor Importance	Less toxic than Inorganic As(III)
<i>Pentavalent Arsenic</i>	As(V)	Aerobic	10 times less toxic than As(III)
Arsenate, Inorganic	H <sub>3</sub> AsO <sub>4</sub> , H <sub>2</sub> AsO <sub>4</sub> <sup>1-</sup> , HAsO <sub>4</sub> <sup>2-</sup> , AsO <sub>4</sub> <sup>3-</sup> .	pH = 0-2 pH = 3-6 pH = 7-11 pH = 12-14	
Methylated As(V) Organo-As(V)		Minor importance	Less toxic than Inorganic As(V)

#### 2.4 Arsenic Mobilization In Ground Water

In a typical aquifer in southern Bangladesh, chemical data imply that arsenic mobilization is associated with recent inflow of carbon. High concentrations of radiocarbon-young methane indicate that young carbon has driven recent biogeochemical processes, and irrigation pumping is sufficient to have drawn water to the depth where dissolved arsenic is at a maximum. The results of field injection of molasses, nitrate, and low-arsenic water show that organic carbon or its degradation products may quickly mobilize arsenic, oxidants may lower arsenic concentrations, and sorption of arsenic is limited by saturation of aquifer materials. (Charles et al., 2002)

## 2.5 Drinking Water Standards Relating To Arsenic

According to ECR 1997, drinking water standard for arsenic in Bangladesh is 50 µg/L (or 0.05 mg/L). The WHO guideline value for arsenic in drinking water is 10 µg/L (or 0.01 mg/L) and the USEPA is also planning to revise its standard from 50 µg/L to 10 µg/L.

## 2.6 Health Effects Of Arsenic

In a population drinking arsenic contaminated water, a great variety of specific as well as non-specific symptoms may be observed. Table 2.2 lists some of the effects of arsenic reported to be due to exposure through drinking water.

Effect	Symptoms	Remarks
Blackfoot Disease Arsenical dermatosis	Dermal lesion, Peripheral neuropathy, Keratosis, Hyperkeratosis, Hyperpigmentation	May necessitate operation
None specific	Nausea, Abdominal Pain, Diarrhoea, Vomiting, Conjunctivitis, Oedema	Mainly due to acute intoxication
Pregnancy disorders	Spontaneous abortions, miscarriages	-
Heart Disease	Coarctation of aorta, Cardiovascular disturb	Among Children
Cancer	Bladder, Kidney, Skin & Lungs, Liver & Colon	-
Mortality	-	Mainly due to Cancer

In a study by the National Institute of Preventive and Social Medicine (NIPSOM), arsenic related diseases (arsenicosis) have been identified in 37 districts (Ahmed et al., 1998). A total of 6000 cases were identified in 162 villages in the 37 districts, mostly in the rural areas. Three stages of manifestations of chronic arsenicosis were observed in the study (Ahmed et al., 1998), but most of the patients were found in the first and second stages. The most common presentations were melanosis, keratosis, hyperkeratosis and depigmentation. Cancers were found among 0.8% and

actinic keratosis and Bowen's diseases were observed among 3.1% of the cases. It is important to note that the study found that the cases at initial and second stages of toxicity showed improvement when patients stopped taking arsenic contaminated water and increased intake of protein rich food, vitamin A, E and C.

## 2.7 Arsenic Contamination Of Groundwater In Bangladesh

In Bangladesh arsenic was first detected in late 1993 in groundwater samples from the district of Chapai Nawabgonj bordering the West-Bengal district of India. Since then higher levels of arsenic have been detected in many regions of the country. The British Geological Survey (BGS) in cooperation with the Department of Public Health Engineering (DPHE) (BGS/DPHE, 2001) carried out the most comprehensive study on distribution of arsenic in groundwater of Bangladesh. In this study, water samples from 3534 tubewells from 61 out of 64 districts and from 433 out of the 496 upazillas were analyzed. Recently, the Bangladesh Arsenic Mitigation Water Supply Project (BAMWSP) carried out a detailed screening of tubewells and survey of arsenicosis patients in 270 arsenic affected upazillas of the country (BAMWSP, 2005). In this study, every household of these arsenic-affected upazillas was surveyed and all tubewells were tested using field test kits. A total of 4,946,933 tubewells were screened for arsenic and over 66 million people surveyed for arsenicosis.

The regional pattern of arsenic distribution obtained from the BGS/DPHE and BAMWSP surveys are very similar, with the greatest contamination in the south and south-east (except Chittagong and Chittagong Hill Tracts) region and least in the north-west and in the uplifted areas of the north central Bangladesh. Figure 2.4 shows the distribution of arsenic concentration in Bangladesh based on the nationwide survey carried out by BGS/DPHE. According to BGS/DPHE (2001) arsenic concentration exceeding the Bangladesh standard of 50 ppb was detected in 53 out of 61 districts, and in 249 upazillas out of 433 sampled upazillas. Out of 3534 samples, only 9% were from deep (>150m) tubewells and the rest were from shallow wells. Among the shallow tubewells, 27% contained arsenic in excess of 50 ppb and

46% in excess of WHO guideline value. For the deep tubewells, the corresponding figures are 1% and 5% respectively (BGS/DPHE, 2001). The survey results revealed some 'hot spots' with high arsenic concentration in some least contaminated regions (e.g., Chapai Nawabgonj in western Bangladesh).

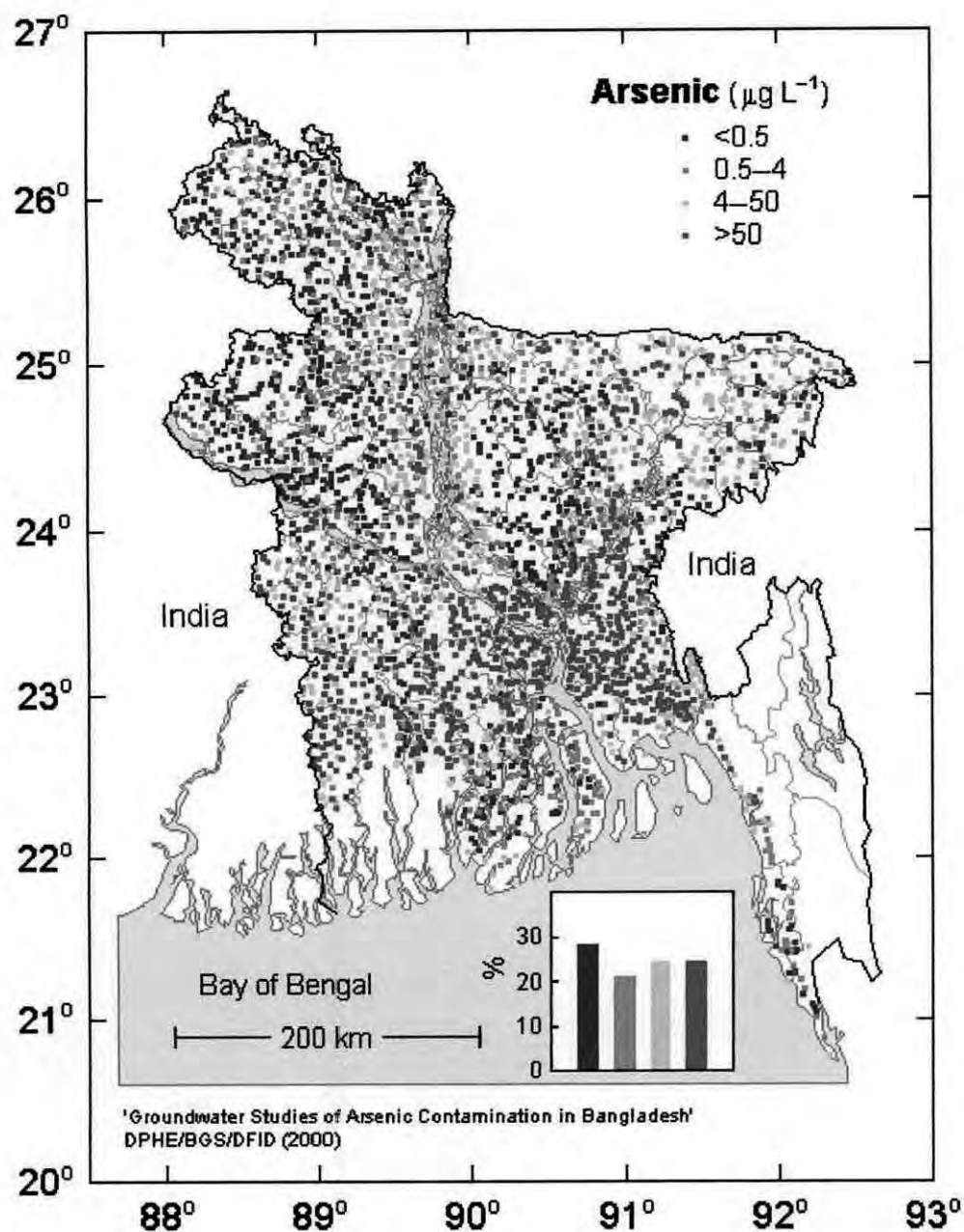


**Figure 2.4:** Distribution of arsenic concentration in Bangladesh based on the nationwide survey carried out by BGS/DPHE.

It was recognized that the sample density in the BGS/DPHE survey was not sufficient to ensure detection of all such 'hot spots'. An important observation from this and other arsenic surveys is the significant variation of arsenic concentration in well waters within short distances. Neighboring wells within a village have been found to contain quite different concentrations of arsenic and other water quality parameters (BGS/DPHE, 2001). In the vertical dimension, high concentrations have been detected within tens of meters of low concentrations.

Estimates of population exposed to arsenic concentration above the Bangladesh drinking water standard of 0.05 mg/L vary from about 20 million to over 36 million (DPHE/BGS/MML, 1999; EES/DCH, 2000; Begum, 2001; BGS/DPHE, 2001). According to BGS/DPHE (2001), 35 million people of Bangladesh are exposed to an arsenic concentration in drinking water exceeding the national standard of 50  $\mu\text{g/L}$  and 57 million people exposed to a concentration exceeding the WHO guideline value of 10 $\mu\text{g/L}$ .

Yu et al. (2003) estimated that if consumption of contaminated water continues, the prevalence of arsenicosis and skin cancer in Bangladesh will be approximately 2,000,000 and 1,000,000 cases per year, respectively and the incidence of death from cancer induced by arsenic will be approximately 3,000 cases per year. In the nationwide screening program carried out by the BAMWSP, over 66 million people of every household of 270 arsenic-affected upazillas were surveyed for arsenicosis patients. Figure 2.5 shows the distribution of arsenicosis patients in the survey areas. A total of 38,430 arsenicosis patients were identified in this survey. Results from all previous surveys show poor correlation between the percentage of contaminated groundwater in a particular area and the density of patients (BGS/DPHE, 2001). Although the BAMWSP survey shows relatively low prevalence of arsenicosis, many fear it to be the 'tip of the iceberg', considering the usual delayed effect of arsenic on exposed population.

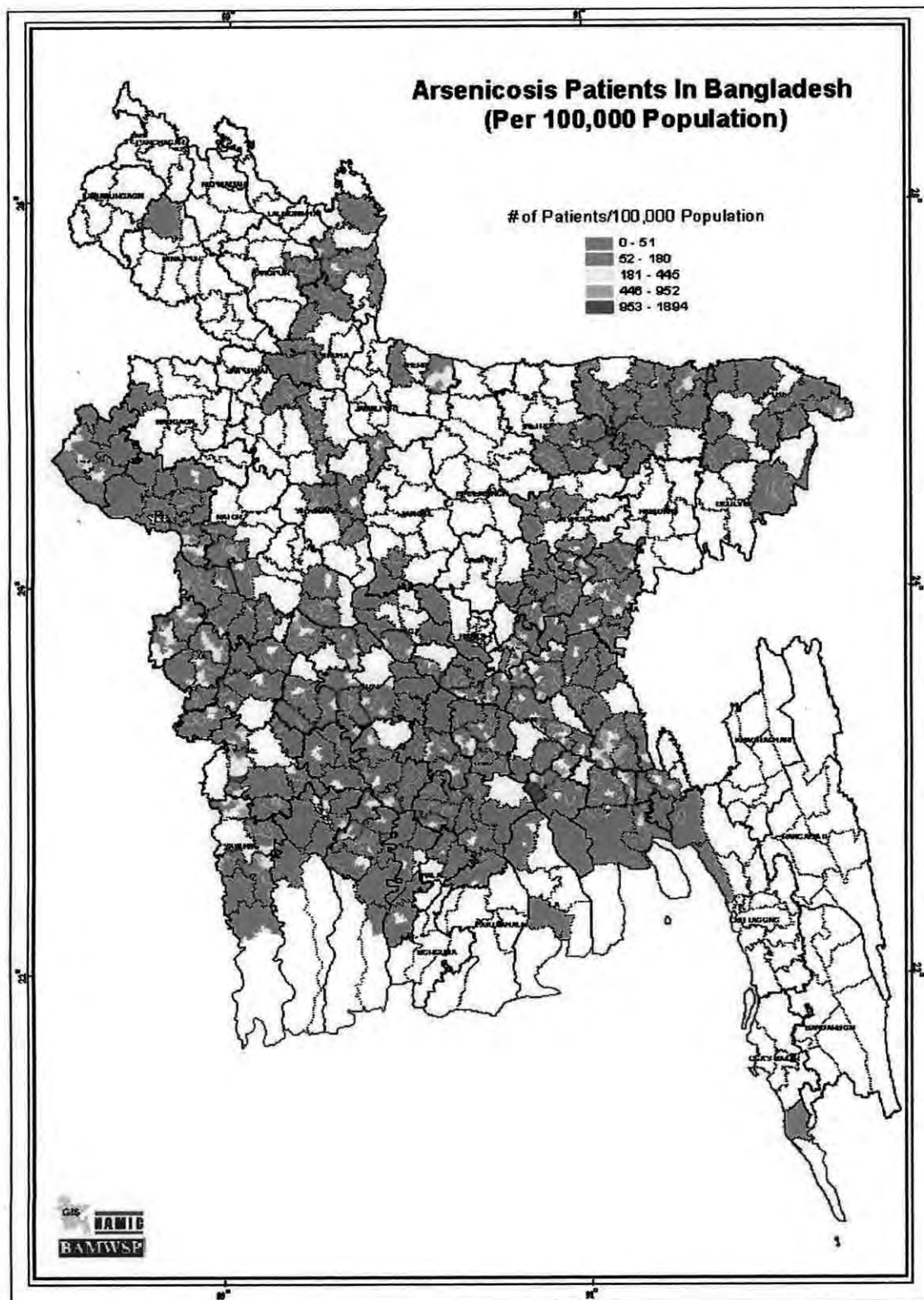


**Figure 2.5:** Distribution of Arsenicosis Patients in Bangladesh.

(Source: BAMWSP, 2005)

## 2.8 Inherent Limitations Of Existing Techniques Used For Arsenic Removal From Water

A wide range of adsorbents are available commercially which are used for arsenic removal from groundwater. Each of the methods involving these adsorbents have their own advantages and disadvantages. These methods include anion exchange resins, adsorbents like activated alumina, granular iron oxide-based media, granular zirconia, granular titania, and iron flocculation processes (Driehaus et al., 1998; Berdal et al., 2000; Rubel, 2003a; Badruzzaman and Westerhoff, 2005).

### 2.8.1 Anion Exchange Resins

Conventional polymeric anion exchanges have a low selectivity for arsenate, and thus the high concentration of sulfate in drinking water successfully competes with arsenate for available anion exchange sites resulting in a short operational life. In an experimental study, increasing the sulfate concentration from 50 to 200 ppm caused the number of bed volumes of water treated before arsenic breakthrough to decrease from approximately 900 to 200 (Rubel, 2003b). This bed life compares very unfavorably with many of the adsorptive media where bed life is typically measured in thousands or tens of thousands of bed volumes (Amy et al., 2000). As a result, ion exchange resins need to be frequently regenerated, resulting in large volumes of an arsenic-laden brine, which needs to be disposed of. In addition, conventional ion exchange resins will not remove uncharged  $\text{H}_3\text{AsO}_3$ , so some form of preoxidation is required in instances where the arsenic is present predominantly as As(III).

### 2.8.2 Activated Alumina/ Iron Coated Sand

Adsorbents like activated alumina or iron coated sand are popularly used for arsenic removal. However these technologies also have their inherent weakness. Conventional Activated Alumina has ill-defined pore structures, low adsorption capacities and exhibits slow kinetics. The adsorbent material needs replacement after 4-5 regenerations. Also the iron-coated sand used as arsenic adsorbent is not standardized and produces toxic solid waste, which requires specific attention for disposal.

### 2.8.3 Granular Iron Oxide-Based Media

Many of the granular iron oxihydroxide-based, porous media have a very high affinity for arsenate and a negligible affinity for other common anions, such as sulfate, bicarbonate, and chloride (Meng et al., 2000), which means that they have operational lives measured in tens of thousands of bed volumes in many cases. However, a major drawback, which is causing operational problems, is the low structural stability of many of the granular media (North, 2005). In use, the media requires periodic backwashing to remove fines generated from the breakdown of the media granules. This backwash solution needs to be treated and safely disposed of, and additional capital equipment needs to be installed to facilitate the backwash process. The EPA highlighted these issues in recent reports. At Desert Sands, NM, an arsenic removal system utilizing one commercial iron oxide media needed to be backwashed 22 times over a 6-month period due to pressure buildup across the media beds (Coonfare et al., 2005). Similar problems were also reported at a system in Rollinsford, NH, where backwashing was frequently required to remove fines that had caused excessive pressure drops across the media beds (Oxenham et al., 2005). These granular media cannot be regenerated due to their low physical strength.

### 2.8.4. Iron Flocculation Process

Coagulation using iron floc as a treatment method is highly effective at removing arsenic from water but generates large amounts of a ferric hydroxide floc which will require safe disposal in a landfill. Capital equipment requirements are generally high, since a ferric hydroxide floc can be difficult to separate from solution effectively. Although chemical consumption is low, ferric floc systems require high levels of maintenance and are generally best suited to large municipal authorities where large volumes of water are being treated daily at a single location, making the system more cost effective.

### 2.8.5. Membrane Techniques

Membrane techniques include highly efficient methods like Nanofiltration, Reverse osmosis, Electrodialysis. These methods are well defined and have high removal efficiency. Reverse osmosis usually produce no toxic solid waste and Electrodialysis



are capable of removing other contaminants in addition to arsenic. However the main drawbacks in applying these techniques are they require very high capital and running cost, pre-conditioning. Nanofiltration technique has high water rejection and Electrodialysis produces toxic wastewater.

## 2.9 Surface Area Of Common Adsorbents

Adsorbents like activated alumina, iron coated sand, MnO<sub>2</sub>, TiO<sub>2</sub>, Goethite, etc. are used in existing arsenic removal techniques. The surface area of adsorbent is an important parameter to assess its effectiveness for removal of contaminants. Surface area of these adsorbents has been reported in previous research works. Table 2.3 shows the specific surface area of some common adsorbents used in developing arsenic removal system.

<b>Table 2.3: Specific Surface Area (SSA) of common adsorbents used for As Removal</b>		
Adsorbent	Specific Surface Area (m <sup>2</sup> /g)	Reference
Activated Alumina	200-300	Chen et al., 2004
Iron Coated Sand	17	Ko et al., 2007
MnO <sub>2</sub>	23	Ouvrard et. al., 2005
Goethite	20	Hongshao et al., 2001
TiO <sub>2</sub>	50	Lee and Choi, 2002

## 2.10 Use Of Iron Nanoparticles For Arsenic Removal

Despite their minuscule status, nanoscale particles may hold the potential to cost-effectively address some of the challenges of site remediation (Masciangioli and Zhang, 2003; EPA, 2003). Two factors contribute to the nanoparticles' capabilities as an extremely versatile remediation tool. The first is their small particle sizes (1–100 nm). In comparison, a typical bacterial cell has a diameter on the order of 1 μm (1000 nm). Nanoparticles can be transported effectively by the flow of groundwater. Due to this attribute, the nanoparticle-water slurry can be injected under pressure

and/or by gravity to the contaminated plume where treatment is needed. The nanoparticles can also remain in suspension for extended periods of time to establish an *in situ* treatment zone. Equally important, they provide enormous flexibility for both *in situ* and *ex situ* applications. For example, nanoparticles are easily deployed in slurry reactors for the treatment of contaminated soils, sediments, and solid wastes. Alternatively, nanoparticles can be anchored onto a solid matrix such as activated carbon and/or zeolite for enhanced treatment of water, wastewater, or gaseous process streams.

The iron oxide nanoparticles can act as an integral component of active nanostructures for targeted delivery of reactive nanomaterials to subsurface contaminants. These nanomaterials can also act together while impregnated into a matrix as a filtering media for arsenic removal. The use of ArsenX $np$ , a hybrid inorganic/organic sorbent that has been developed for the removal of arsenic from drinking water, is a good example of the application of iron oxide nanoparticles used as a filtering media. ArsenX $np$  consists of hydrous iron oxide nanoparticles impregnated into 300–1200 $\mu\text{m}$  durable polymeric beads. The nanosize of the hydrous iron oxide particles results in a very high surface area, and this, coupled with the high porosity of the polymer substrate, ensures that the rate of arsenic uptake is, at least initially, relatively rapid, and the arsenic removal capacity is high. In addition to the kinetics of surface adsorption, the rate and effectiveness of arsenic uptake will depend later in the process upon the mass transfer of arsenic (and other anionic species present) into the resin bead. This means that a column of ArsenX $np$  only requires a contact time of between 2 and 3 min for optimum arsenic uptake as opposed to the 4–5 min required for optimum performance of a typical granulated iron media (Siegel et al., 2006). Siegel et al., 2006 showed that the operating capacity of a granulated iron media was significantly increased when the contact time with the iron oxide was increased from 2 to 5 min.

Recent research has suggested that as a remediation technique, nanoscale iron particles have several advantages: (1) effective for the transformation of a large variety of environmental contaminants, (2) inexpensive, and (3) nontoxic.

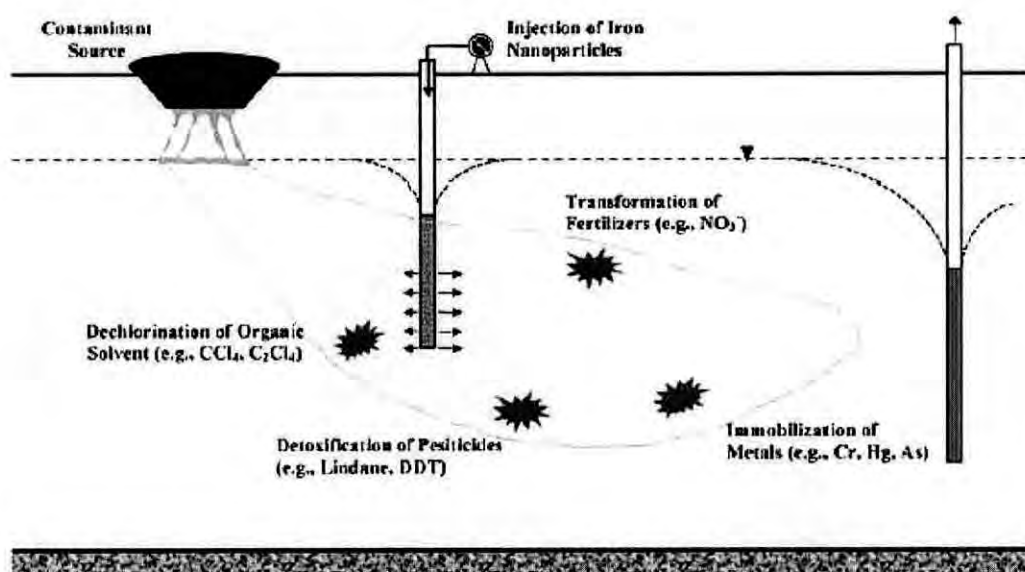


**Figure 2.6:** Nanoscale iron particles for *in situ* remediation.

Direct subsurface injection, whether under gravity-fed or pressurized conditions, has already been shown to effectively transform chlorinated organic compounds (Elliott and Zhang, 2001; Glazier et al., 2003). The technology holds great promise for immobilizing heavy metals and radionuclides as well. Examples of potential applications of nanoscale iron particles for site remediation are further illustrated in Figure 2.6.

Permeable reactive barriers (PRBs) are a recent development of a passive system to remediate subsurface waters containing organic or inorganic contaminants. Contaminated groundwater flows under its natural gradient and passes through a permeable curtain (Figure 2.7) of treatment medium that either; (i) removes the contaminants from the aqueous phase by one or several mechanisms or (ii) transforms the contaminants into environmentally acceptable or benign species. The most widely adopted treatment medium is elemental iron ( $\text{Fe}^0$ ), a substance that is

highly reactive, environmentally acceptable, and is readily available as a manufactured product derived from the recycling of scrap iron and steel.

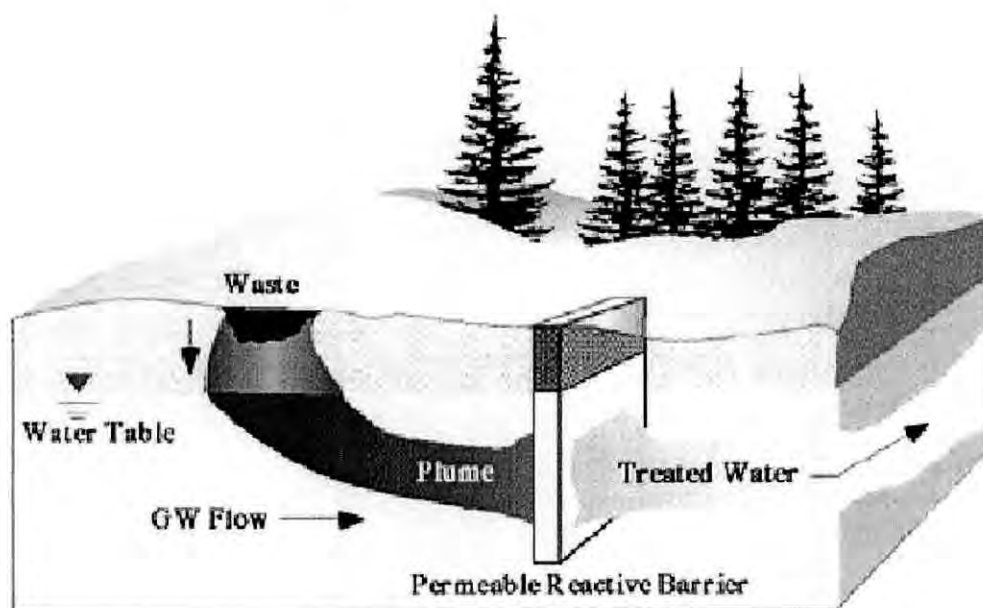


**Figure 2.7:** Illustration of a permeable reactive barrier remediating a plume

(Source: [www.powellassociates.com](http://www.powellassociates.com))

In cores of the reacted treatment media, the most abundant secondary product formed *in situ* is Fe-oxyhydroxide (iron corrosion products – iron hydroxides and oxides) (Noubactep et al., Manuscript in preparation 2008). Nanoparticles impregnated into a solid permeable matrix can also be used as a PRB for treatment of arsenic contaminated water.

The use of magnetite nanoparticles for removal of arsenic from water showed great potential for its possible application as an adsorbent in a filter media. It is therefore important to explore other forms of iron oxide nanoparticles in terms of their arsenic adsorption capacity. Hence the present research work concentrates on understanding the adsorption characteristics of hematite nanoparticles, which is essential for subsequent development of an in-situ or ex-situ treatment system based on these nanoparticles.

### Review of Adsorption of Arsenic on Magnetite Nanoparticles:

Previous works regarding adsorption of arsenic on magnetite nanoparticles (Yean et al., 2005) showed that arsenic adsorption isotherm appeared to consist of two Langmuir type isotherms for both arsenite and arsenate. Figure 4.6 shows the adsorption isotherms for As(III) and As(V) on magnetite nanoparticles (size: 11.72 nm) reported by Yean. It shows that at low concentration, the adsorption isotherms can be fitted with a simple Langmuir Isotherm. However, at high As concentrations, the adsorption data deviates from the simple Langmuir isotherm, and appears to follow a second Langmuir isotherm.

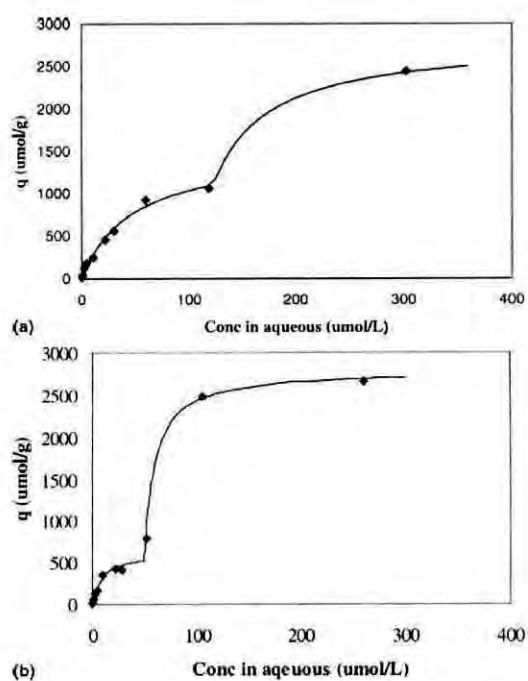


**Figure 2.8** : Adsorption of Arsenic to 11.72 nm magnetite at pH 8.0: (a) As(III) and (b) As(V) (Yean et al., 2005)

### 2.11 Evaluation Of Kinetic Rate Constants Of Adsorption

The kinetics of adsorption of any sorbate on a sorbent can be described by the pseudo first-order and second-order kinetic models. The first-order kinetic model

(Lagergren, 1898) and the second-order kinetic model (Mckay and Ho, 1999) is expressed as follows:

$$\log(q_e - q) = \log q_e - \frac{k_1 t}{2.303} \dots\dots\dots \text{(First-order kinetic model)}$$

$$\frac{t}{q} = \frac{1}{k_2 q_e^2} + \frac{t}{q_e} \dots\dots\dots \text{(Second-order kinetic model)}$$

Where,  $q_e$  and  $q$  ( $\mu\text{M}$ ) are the amounts of sorbate (e.g. like As) adsorbed onto adsorbent at equilibrium and at time  $t$ , respectively.  $k_1$  ( $\text{hr}^{-1}$ ) and  $k_2$  ( $\mu\text{M}^{-1} \text{hr}^{-1}$ ) are the rate constants of first-order and second-order adsorption. The slopes and intercepts of plots of  $\log(q_e - q)$  versus  $t$  were used to determine the first-order rate constant  $k_1$  and  $q_e$ . The slopes and intercepts of plots of  $t/q$  versus  $t$  were used to calculate the second-order rate constant  $k_2$  and  $q_e$ .

## 2.12 Summary

Several research works have been carried out in the past on adsorption desorption characteristics of arsenic on different types of nanoparticles (Yean et al., 2005; Doušová et al., 2006; Zhang, 2003; Sylvester et al., 2007). Although arsenite is the dominant form of arsenic in groundwater of Bangladesh, its adsorption has been found very poor on most common adsorbents. It is very important to carry out research works for better understanding of adsorption characteristics of arsenic (both arsenite and arsenate) on novel adsorbents. As mentioned earlier that the increased surface area of the nanoparticles make it an effective adsorbents for arsenic. However it is important to investigate other water quality parameters like pH, presence of phosphate, which may influence the targeted arsenic adsorption and reduce the arsenic removal efficiency of the adsorbent. Controlled experiments need to be carried out to better understand the processes leading to arsenic adsorption on iron oxide nanoparticles.

---

## CHARACTERIZATION OF THE HEMATITE NANOPARTICLES

### 3.1 Introduction

Nanoscale iron oxide particles represent a new generation of environmental remediation technologies that could provide cost-effective solutions to some of the most challenging environmental cleanup problems. Nanoscale iron oxide particles have large surface areas and high surface reactivity. Equally important, they provide enormous flexibility for *in situ* applications. Research has shown that nanoscale iron oxide particles are very effective for the transformation and detoxification of a wide variety of common environmental contaminants, such as chlorinated organic solvents, organochlorine pesticides, and polychlorinated biphenyls (PCBs) (Zhang, 2003). Modified iron oxide nanoparticles, such as catalyzed and supported nanoparticles have been synthesized to further enhance the speed and efficiency of remediation (Zhang, 2003).

In this study the hematite ( $\text{Fe}_2\text{O}_3\text{-}\alpha$ ) nanoparticles were assessed as an adsorbent for arsenic removal. Nanostructured and Amorphous Materials, Inc. (16840 Clay Road, Suite 113 Houston, TX 77084, USA) commercially produced the hematite nanoparticles. A sample of 500g of Hematite nanoparticles was procured and the basic characteristics of the material provided by the manufacturers are shown in Table 3.1.

However the commercially procured hematite nanoparticles were further analysed in the laboratory. This analysis was done to get reliable data on the composition, structure, size and size distribution of the nanoparticles. Also the surface area per unit weight and the surface charge with varying pH was determined to get a better

understanding of the adsorption mechanism. These results of the laboratory analysis were checked for consistency with those provided by the manufacturer.

<b>Table 3.1:</b> Details of commercially procured hematite nanoparticles	
<i>Iron Oxide (Fe<sub>2</sub>O<sub>3</sub>, alpha)</i>	
Purity:	98+ %
Apparent Particle Size (APS):	20-50 nm
Specific Surface Area (SSA):	~50 m <sup>2</sup> /g
Color:	Red Brown
Morphology:	Spherical
Bulk density:	1.20 g/cm <sup>3</sup>
True density:	5.24 g/cm <sup>3</sup>

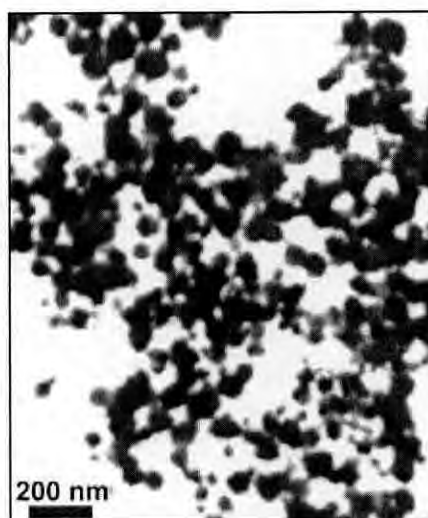


**Figure 3.1:** TEM image of Hematite Nanoparticles.

(Source: Nanostructured & Amorphous Materials, Inc.)

## 3.2 Methodology For Physical Characterization Of Hematite Nanoparticles

### 3.2.1 Potentiometric Titration of Hematite Nanoparticles

The surface charge of hematite nanoparticles was determined under different pH values by potentiometric titration. The PZC (pH of zero surface charge) was also determined from titration data. Potentiometric titration of 0.5g/L of hematite suspensions was conducted in 0.01 M and 0.10 M aqueous solution of NaNO<sub>3</sub> as the background electrolyte. Standard HCl (0.05 M) and NaOH (0.05 M) solutions were used for titration.

The experimental protocol for the titration test consisted of the following steps: (i) Stock solution of NaNO<sub>3</sub> (concentration: 1.0 M) was prepared. (ii) The aqueous solutions were prepared by adding required quantities (1ml or 10ml) of NaNO<sub>3</sub> stock solution in a 100 ml volumetric flask. (iii) The flask was filled with distilled water upto the 100ml mark. This way two different concentration of background



electrolytes (0.01M and 0.10M) were prepared. After preparation of the final solution it was taken into a 150ml glass beaker. (iv) 0.05 g of hematite nanoparticle was added in the solution to get a final concentration of 0.5g/L of hematite. (v) At the beginning of each experiment the hematite nanoparticles were dispersed in solution by sonication using a sonication probe (Sonifier®, Branson Sonic Power Company Danbury, Connecticut, Power Supply, B-12.) for 10 min. (vi) After sonication the sample pH was measured and an equilibration period was allowed so that the pH value remained fixed for about one minute. (vii) Then required amount of 0.05M HCl or 0.05M NaOH solution was added to the solution using a micropipette and the suspension was stirred with a magnetic stirrer for 10 minutes. (viii) After that the solution pH was measured again in the same way as mentioned in step (vi). (ix) Step (vii) and (viii) were repeated consecutively until a pH range of 3 to 10 was obtained.

For one concentration of background electrolyte, titration by 0.05M HCl and 0.05M NaOH were carried out in duplicate.

### 3.2.2 X-ray Diffraction (XRD) analysis

X-ray Powder Diffraction (XRD) is an efficient analytical technique used to identify and characterize unknown crystalline materials. Monochromatic x-rays are used to determine the inter-planar spacing of the unknown materials. Samples are analyzed as powders with grains in random orientations to insure that all crystallographic directions are "sampled" by the beam. When the Bragg conditions for constructive interference are obtained, a "reflection" is produced, and the relative peak height is generally proportional to the number of grains in a preferred orientation.

The X-ray spectra generated by this technique, thus, provide a structural fingerprint of the unknown. Mixtures of crystalline materials can also be analyzed and relative peak heights of multiple materials may be used to obtain semi-quantitative estimates of abundances.

In this research work the XRD analysis of the procured hematite nanoparticle was performed at the laboratory of Bangladesh Atomic Energy Commission (BAEC), Dhaka to analyze the composition of the hematite nanoparticles. The XRD analysis was conducted with a *Philips X'Pert Pro X-ray Diffractometer* at 40kV and 30mA. It used copper  $K\alpha$  radiation and a graphite monochromator to produce X-rays with a wavelength of 1.54060 Å. Hematite nanoparticles were placed in a 10mm specimen length and scanned from 15° to 70°. This scan range covered all major species of iron and iron oxides. The scanning rate was set at 2.0°/min (Step Size,  $2\Theta = 0.02$ , Scan Step Time, sec = 0.60).

### 3.2.3 BET (Brunauer-Emmett-Teller) surface area analysis

Determination of specific surface area of nonporous solids such as hematite,  $N_2$  gas adsorption and BET analysis of the resulting isotherm is the most popular experimental method. Effective surface area of the iron nanoparticles was estimated using Brunauer-Emmett-Teller (BET) physisorption method (Braunauer et al., 1938). For the present study, Dr. Navid Bin Saleh (currently an Assistant Professor at University of South Carolina, USA) carried out the BET surface area analysis in the laboratory of Yale University, where he worked as a Post-doctoral Research Associate.

Nitrogen adsorption-desorption isotherms were measured at -196 °C using a static volumetric instrument Autosorb-1C (Quanta Chrome, Boynton Beach, FL). Prior to the measurement, the samples were out-gassed at 300 °C to a residual pressure of  $5 \times 10^{-3}$  Torr. The pore size distributions were estimated from the desorption isotherms using the BJH model (Barrett et al., 1951).

### 3.2.4 DLS (Dynamic Light Scattering) analysis

Dynamic Light Scattering (also known as Photon Correlation Spectroscopy) is one of the most popular methods used to determine the size of particles. Shining a monochromatic light beam, such as a laser, onto a solution with spherical particles in Brownian motion causes a Doppler Shift when the light hits the moving particle, changing the wavelength of the incoming light. This change is related to the size of

the particle, and makes it possible to compute the sphere size distribution and give a description of the particle's motion in the medium, measuring the diffusion coefficient of the particle and using the autocorrelation function. For the present study Dr. Navid Bin Saleh (currently an Assistant Professor at University of South Carolina, USA) carried out the DLS analysis in the laboratory of Yale University, where he worked as a Post-doctoral Research Associate.

For DLS Analysis stock solution of the hematite nanoparticle suspension was prepared in de-ionized water. Three test runs were made on hematite samples. These consist of the following;

- 1) At first the particle size of hematite was observed in de-ionized water after sonicating for 10 minutes.
- 2) Aggregation of the nanoparticles was observed after adding 10mM NaNO<sub>3</sub> in the solution as background electrolyte to commence aggregation.
- 3) Aggregation of the nanoparticles was observed after adding 10mM NaNO<sub>3</sub> and 50mM MES or HEPES in the solution to commence aggregation.

The aggregation experiments were performed using a multiangle light scattering unit (ALV-5000, Langen, Germany) equipped with a solid-state Nd:vanadate (Nd:YVO<sub>4</sub>) laser (Verdi V2, Coherent, Santa Clara, CA) providing a single-frequency output of 532nm. Further details of the instrument are described elsewhere (Chen et al., 2007). The iron nanoparticle samples were placed in new glass vials (Supelco, Bellefonte, PA) that were previously soaked in a cleaning solution (Extran MA 01, Merck KGaA, Darmstadt, Germany) overnight, thoroughly rinsed in deionized water, and oven-dried under dust-free conditions (Saleh et al., 2008). Electrolyte solutions, pH adjusting reagents, and biological buffers were added prior to the aggregation experiments following the protocol described by Chen and Elimelech (Chen and Elimelech, 2006 and Chen et al., 2006). The dynamic light scattering measurements were conducted by positioning the detector at 90° with the incident laser beam and the autocorrelation function having been allowed to accumulate for over 15 sec. The measurements were performed for a time period ranging from 20

min to 3 h to obtain an approximately 30% increase in the original hydrodynamic radius of the iron nanoparticles (Saleh et al., 2008).

### 3.3 Results And Discussion

#### 3.3.1 Size and Distribution of Hematite Nanoparticles

The size and distribution of Hematite nanoparticles in suspension during the adsorption of arsenic holds great importance in assessing their efficiency as an adsorbent. Although the size determined from XRD analysis (discussed in Section 3.3.3) gives the actual grain size of the NPs, the actual size of the NPs in suspension might vary greatly with that obtained from XRD analysis. Factors like surface charge, pH may play vital role in aggregation of the NPs and cause their effective size to increase substantially.

In the DLS analysis different conditions were applied to assess the aggregation rate of the HNPs in suspension and the results are shown in Figures 3.2, 3.3 and 3.4.

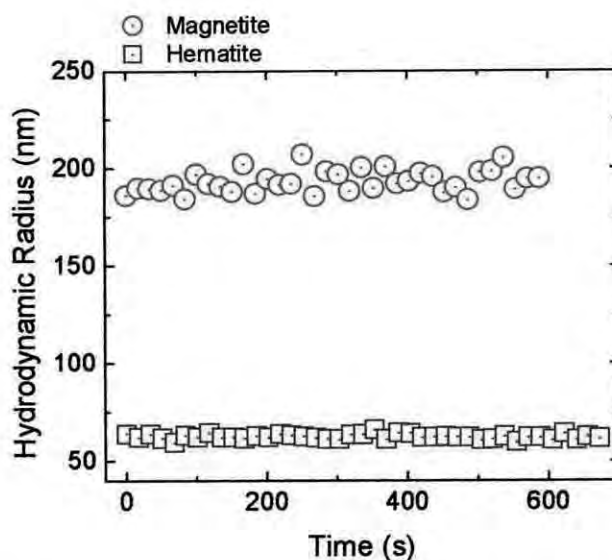


**Figure 3.2:** Average hydrodynamic radius of magnetite and hematite nanoparticle aqueous suspensions. The concentration of the suspensions was 10 mg/L. (Tests carried out at Yale University, New Haven, USA)

Figure 3.2 shows the variation in the Hydrodynamic Radius ( $R_h$ ) of HNPs in aqueous suspension with time. Here the average hydrodynamic radius of HNPs is measured as  $62.1 \pm 1.3$  nm. Temperature for all EPM measurements was kept at 24 °C. It is seen that even after sonication the size of the nanoparticles remain substantially higher in aqueous suspension.

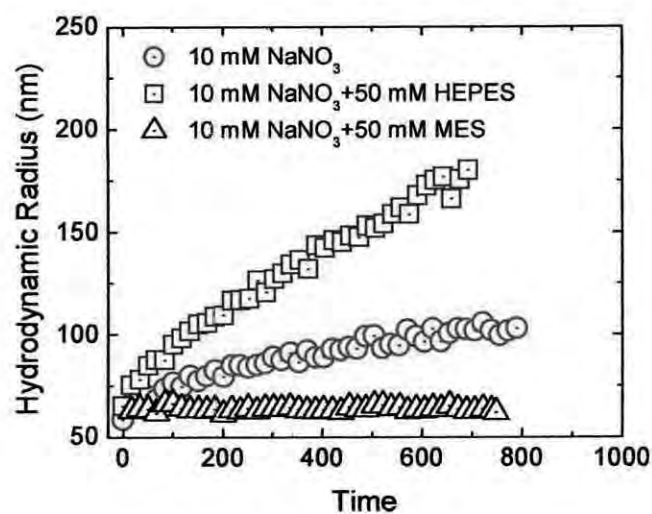


**Figure 3.3:** Aggregation profiles of hematite NPs with and without the biological buffers. (Tests carried out at Yale University, New Haven, USA)

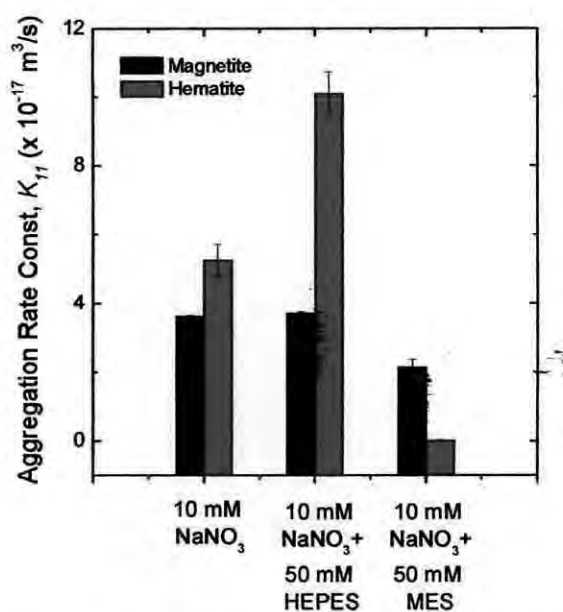


**Figure 3.4:** Aggregation rate constants of magnetite and hematite NPs with and without biological buffers. (Tests carried out at Yale University, New Haven, USA)

The grain size of the HNP determined from XRD was 31.5nm and the  $R_h$  of the sample shows that the effective diameter is 134.2 nm, which is more than four times the actual grain size.

Figure 3.3 shows the aggregation of the HNPs with time in different solutions with and without biological buffers. The buffer solutions were added immediately prior to commencing the aggregation experiments and the experiments were carried out at room temperature (23 °C). It is seen that while using MES (i.e. pH 5.15) the particle size remained almost constant with time. The  $pH_{PZC}$  value referred in literature (Plaza et al., 2001) is 7.3 and the pH of zero surface charge determined in present research is around 6.5. The size stability of the HNPs at pH 5.15 can be attributed to the fact that at this pH value the common positive charge on the surface cause electrostatic repulsion and hence the particles do not aggregate with time. However as the pH value increases the surface group deprotonation increases and will finally reverse the charge into a negative one. During this change, the degree of destabilization will be a maximum due to charge neutralization (Adachi et al., 2005). Hence the aggregation of the HNPs was fastest in case of using HEPES buffers (pH 7.5). In case of no biological buffers gradual aggregation took place with a background electrolyte of 0.01M  $NaNO_3$ .

The aggregation rate constants in Figure 3.4 were calculated based on initial aggregation of the HNPs. Here it is also seen that the aggregation rate was less while using MES (pH 5.15) and more while using HEPES (pH 7.5).

### 3.3.2 Specific Surface Area of Hematite Nanoparticles

The BET specific surface area measurement of the hematite nanoparticles was performed along with another sample of magnetite nanoparticles and the results obtained are shown in Table 3.2.

Table 3.2: Estimated surface area of the iron nanoparticles using BET method	
Particle Type	Surface Area (m <sup>2</sup> /g)
Magnetite	37.7
Hematite	13.8

Here the surface area determined by the BET test is different from the one mentioned by the manufacturers. However the sample test results are more acceptable than those mentioned. The N<sub>2</sub> adsorption isotherm shows that with increasing partial pressure the adsorbed N<sub>2</sub> volume initially increased at a very small rate and finally the adsorbed volume reached 100cc N<sub>2</sub> per gram of hematite at a partial pressure of unity.

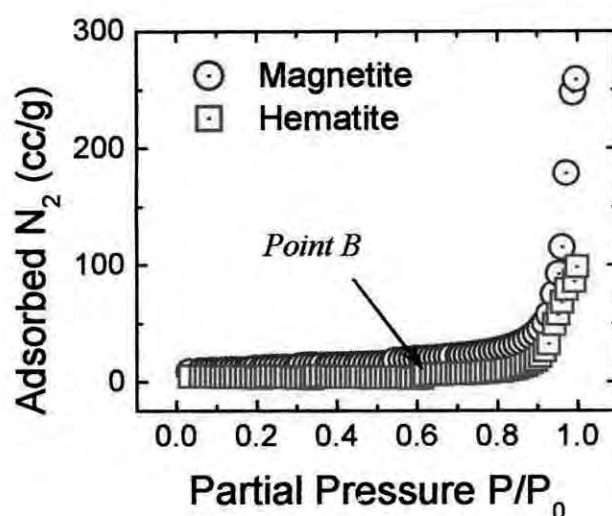


**Figure 3.5:** Adsorption isotherm of N<sub>2</sub> to the iron nanoparticles. The samples were degassed up to  $5 \times 10^{-3}$  Torr at 300 °C. (Tests carried out at Yale University, New Haven, USA)

The isotherm in this case, showed in Figure 3.5, takes the form of a reversible Type II isotherm, which is the normal form of isotherm obtained with a non-porous or macroporous adsorbent. The Type II isotherm represents unrestricted monolayer-multilayer adsorption. *Point B*, the beginning of the almost linear middle section of the isotherm, is often taken to indicate the stage at which monolayer coverage is complete and multilayer adsorption about to begin (Sing et al., 1985). In case of

Hematite nanoparticles the *Point B* is observed at a Partial Pressure of 0.6, and after that multilayer adsorption takes place with increasing partial pressure.

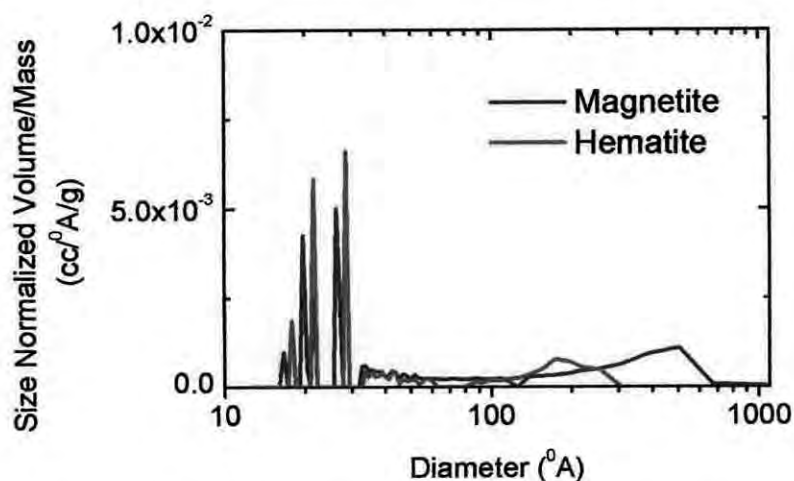


**Figure 3.6:** Pore size distribution of iron nanoparticles.  
(Tests carried out at Yale University, New Haven, USA)

The pore size distribution of the hematite nanoparticles generated using BJH model while desorbing  $N_2$  from particle surfaces are shown in Figure 3.6. The particles have internal pore size at 18-30 Å diameter range, with maximum internal pores size of around 22 Å and 28 Å diameters. These pore size is an important piece of information as adsorption takes place by filling up the pore space of the particles.

### 3.3.3 Structure and Composition of Hematite Nanoparticles

Figure 3.7 is the XRD spectrum of the laboratory-synthesized hematite, which confirms the hematite crystal structure as analyzed in previous works (He et al., 2008). The broad attenuated peaks reveal the existence of an amorphous phase of iron. Apparent peaks at the  $2\theta$  of  $33^\circ$ ,  $35.8^\circ$ ,  $41^\circ$ ,  $49.6^\circ$ ,  $54^\circ$ ,  $62.5^\circ$  and  $64.15^\circ$  indicate the presence of Hematite ( $\alpha\text{-Fe}_2\text{O}_3$ ). The mean grain size obtained from the XRD analysis was 31.5 nm.

For a spherical particle with a diameter of  $d$ , the specific surface area (SSA) can be calculated by the following equation:



$$SSA = \frac{\text{SurfaceArea}}{\text{Mass}} = \frac{\pi d^2}{\rho \frac{\pi}{6} d^3} = \frac{6}{\rho d}$$

where  $\rho$  is the density ( $5240 \text{ kg/m}^3$  for hematite) of the solid particle. The theoretical SSA for 31.5 nm particles is therefore  $36,350 \text{ m}^2/\text{kg}$  or  $36.35 \text{ m}^2/\text{g}$ . However this specific surface area determination is based on the fact that the particles are spherical in shape and the mean grain size determined from the XRD analysis was therefore taken as the diameter of the particle. However the data obtained on surface area from the BET analysis ( $13.8 \text{ m}^2/\text{g}$ ) should be taken to be more precise, as in case of BET analysis the shape of the particle was not considered and surface area was determined on the basis of  $\text{N}_2$  adsorption on the surface of hematite nanoparticles.

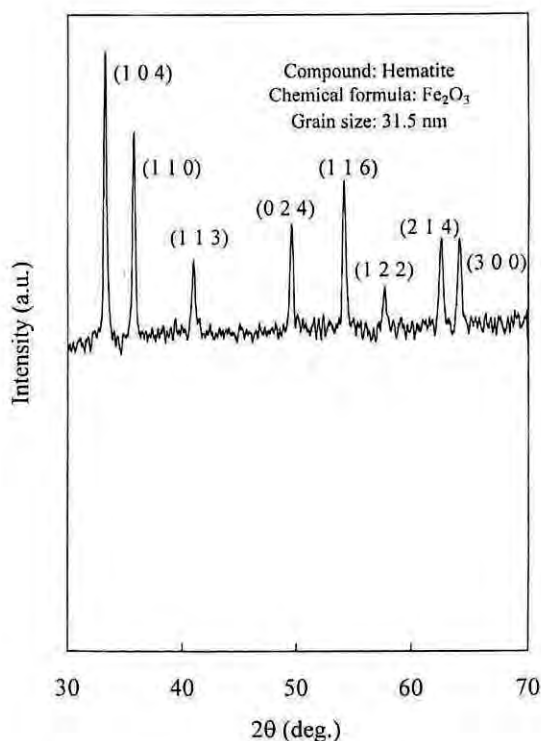


**Figure 3.7:** XRD pattern of Hematite Nanoparticles.  
(Tests carried out at AEC Laboratories, Dhaka)

3.3.4 Surface Charge of Hematite Nanoparticles as a function of pH

The potentiometric titration of the 0.5 g/L hematite nanoparticle using 0.05 M HCl and 0.05 M NaOH provided the necessary data to determine the surface charge at different pH values. The pH versus surface charge for hematite samples is plotted in Fig. 3.8. The surface charge  $\sigma$  was calculated as a function of pH from potentiometric titration data based on Eq. (3.1) (Stumm and Morgan, 1981)

$$\sigma \text{ (C m}^{-2}\text{)} = F (C_A - C_B + [\text{OH}^-] - [\text{H}^+]) a^{-1} S^{-1} \dots\dots\dots (3.1)$$

where  $F$  is the Faraday constant (96,485 C/mol),  $C_A$  and  $C_B$  are the total concentrations of acid and base added, respectively (mol/L),  $[\text{H}^+]$  is the proton concentration (mol/L) given by  $10^{-\text{pH}}/\gamma^{\text{H}^+}$ ,  $[\text{OH}^-]$  is the  $\text{OH}^-$  concentration (mol/L) given by  $10^{-(\text{pK}_w-\text{pH})}/\gamma^{\text{OH}^-}$ ,  $a$  is hematite concentration (g/L), and  $S$  is the specific surface area ( $\text{m}^2/\text{g}$ ). The potentiometric titration curves are showed in Figure 3.9.

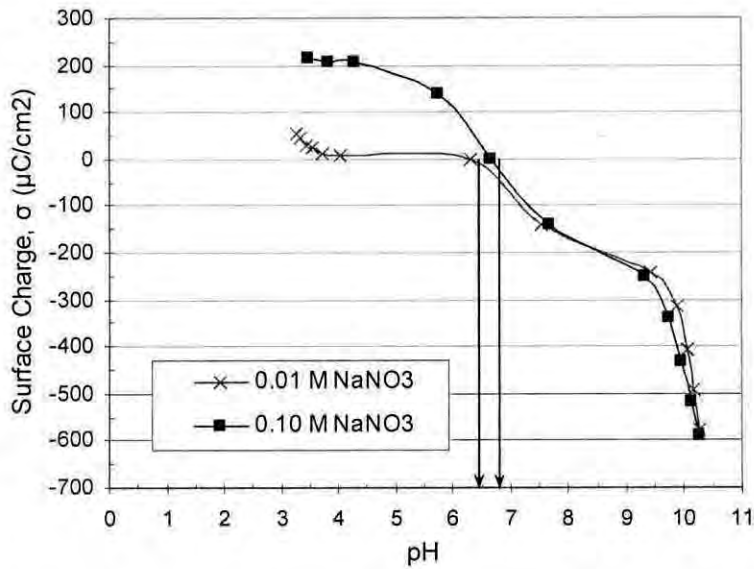


**Figure 3.8:** Surface Charge Density of hematite nanoparticles as a function of pH

The point of zero charge ( $\text{pH}_{\text{pzc}}$ ) is defined as the pH value at which  $\sigma = 0$ . Both hematite samples with background electrolyte concentration of 0.01M and 0.10M of  $\text{NaNO}_3$  have there  $\text{pzc}$  values around pH 6.5. The results of  $\text{pH}_{\text{pzc}}$  obtained in this

research are close to the pH 7.3 from the literature (Plaza et al., 2001). The variation of surface charge with pH plays an important role in the adsorption of arsenic onto hematite nanoparticles.

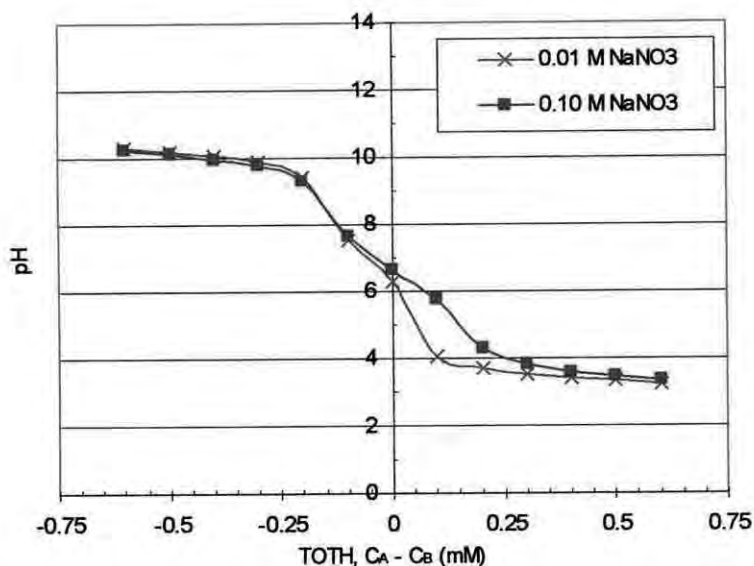


**Figure 3.9:** Potentiometric Titration Curves (pH versus TOTH, mM)

The charge of the predominant oxidation states of arsenic in aqueous solution together with the charge on the hematite surface plays a vital role on the overall adsorption process. Also the pH value near the  $pH_{pzc}$  region is responsible for instability of the hematite nanoparticles. When there is no surface charge on the hematite nanoparticles the Van Der Waal's inter particle force of attraction governs and agglomeration takes place, resulting in increased particle size and less effective surface area for adsorption.

### 3.4 Summary

The characterization of the hematite nanoparticles was an essential part of the overall assessment of hematite as an effective adsorbent for arsenic. Since the nanoparticles were procured from commercial sources, it was very important to check the physical parameters mentioned by the vendor. An important discovery from the characterization tests was the anomaly in the specific surface area determined from

the test results. The specific surface area determined from the BET test was  $13.8\text{m}^2/\text{g}$ , which is well below the mentioned value of  $50\text{m}^2/\text{g}$ . This decreased value of surface area has implication for arsenic adsorption from solution.

The XRD analysis was done to assess the composition of the nanoparticles and it showed that the nanomaterials were  $\alpha\text{-Fe}_2\text{O}_3$  (Hematite). The XRD analysis was necessary to investigate the presence of any impurity in the adsorbent. The presence of any impurity can definitely cause differences in the adsorption quantity. However the hematite nanoparticles did not contain any mentionable amount of impurities as showed by the XRD analysis. Also the mean grain size of the hematite nanoparticles determined from the XRD analysis was  $31.5\text{nm}$ , which was within the range mentioned by the manufacturer ( $20\sim 50\text{nm}$ ).

In order to assess the adsorption characteristics the most important aspect of material characterization was the variation of surface charge with changing pH. The point of zero surface charge as determined from the potentiometric titration analysis was around a pH value of 6.5, this  $\text{pH}_{\text{PZC}}$  value is close to those found by other investigators like Plaza et al. ( $\text{pH}_{\text{PZC}}=7.3$ ). The surface charge was positive for pH values less than  $\text{pH}_{\text{PZC}}$ , and was negative for pH values more than  $\text{pH}_{\text{PZC}}$ . The potentiometric titration analysis was therefore necessary in understanding the effect of pH in the adsorption process.

The characterization of the hematite nanoparticles therefore provided us with essential information on physical parameters like size, specific surface area and composition of the hematite nanoparticles. In addition to this the information on variation of surface charge with pH provided important basis for understanding the adsorption of arsenic on hematite nanoparticles.

---

## ADSORPTION OF ARSENIC ON HEMATITE NANOPARTICLES

### 4.1 Introduction

Arsenic derived from natural sources occurs in groundwater in many countries, affecting the health of millions of people. Iron oxides including poorly crystalline oxides, e.g., ferrihydrite, play a significant role in controlling dissolved As concentration and limit the mobility and bioavailability of As(III) and As(V) (Jain et al., 1999). Recent investigations have confirmed that iron nanoparticles and their corrosion products are suitable materials for remediation of both As(III) and As(V) (Kanel et al., 2005, 2006; Manning et al., 2002). As a filtering media the nanoparticles of hydrous iron oxide distributed throughout a porous polymeric bead forms a hybrid sorbent which is effective for arsenic removal (Sylvester et al., 2007). They also provide enormous flexibility for *in situ* applications. Nanoscale iron particles have large surface areas and high surface reactivity. Modified iron nanoparticles, such as catalyzed and supported nanoparticles have been synthesized to further enhance the speed and efficiency of remediation (Zhang, 2003).

With the advent of different iron oxide nanoparticles, it is necessary to determine their adsorption characteristics under various conditions (e.g., varying pH, presence of competing anions) in order to assess their suitability for use in environmental remediation (e.g., heavy metal removal) processes. The adsorption of arsenic on iron oxide nanoparticles like magnetite, goethite has been described in recent literature (e.g. Sylvester et al., 2007; Yean et al., 2005). The magnetite nanoparticles exhibit an increase in adsorption capacity with decreasing size (Yean et al., 2005). Laboratory-synthesized magnetite nanoparticles can remove approximately two hundred times more arsenic than larger commercial materials. Moreover, arsenic is

not readily released from the magnetite nanoparticles, presumably because the binding of the adsorbed arsenic results in the formation of highly stable iron-arsenic complexes (Yean et al., 2005). However, only limited data are available on adsorption characteristics of hematite nanoparticles.

In this study, adsorption characteristics of arsenic (both arsenate and arsenite, which are the principle forms of As in groundwater) on hematite nanoparticles has been assessed in batch experiments carried out with water samples with different known arsenic concentrations. Effect of phosphate content of water on arsenic adsorption has also been assessed. Also kinetics of arsenic adsorption on hematite nanoparticles was evaluated. The effect of pH on adsorption was also analyzed and adsorption envelope was developed. This chapter presents results of these laboratory investigations and their implications on arsenic removal from arsenic-contaminated groundwater using hematite nanoparticles.

## 4.2 Methodology

### 4.2.1 Batch Adsorption Experiments

#### *Adsorption of Arsenic*

Adsorption characteristics of arsenic and phosphate on hematite nanoparticles (HNP) were assessed in batch experiments carried out in 50ml centrifuge tubes. Adsorption capacities of HNP were evaluated by equilibrating known mass of nanoparticle sample with aqueous solutions of varying arsenic (0.1 ppm to 25.0 ppm) concentrations. The amount of HNP added to each 50ml centrifuge tubes was 0.005g, i.e. HNP concentration was 0.1 g/L. As a background electrolyte  $\text{NaNO}_3$  was used with a concentration of 0.01 M.

The pH of the batch adsorption tests were kept constant using biological buffers (MES, HEPES and CHES) and required amount of 1.487 M NaOH. The constant values of pH in the batch adsorption experiments were 5.15, 6.1, 7.5 and 9.3. MES (2-Morpholinoethanesulfonic acid monohydrate) concentration of 0.05 M was used

to keep the pH value constant at 5.15 and 6.1; 0.05 M HEPES (2-[4-(2-Hydroxyethyl)-1-piperazine] ethanesulfonic acid) and 0.05 M CHES (2-(Cyclohexylamino) ethane-sulfonic acid) was used to keep the pH value constant at 7.5 and 9.3, respectively.

The arsenic batch adsorption experiments consisted of the following steps: (i) Stock solutions of As(III) or As(V) (concentration: 1000ppm), NaNO<sub>3</sub> (concentration: 1.0 M), MES or HEPES or CHES (concentration: 0.5 M) were prepared. (ii) Aqueous solutions were prepared by adding required quantities of arsenic (arsenite or arsenate) stock solution, 0.5 ml of NaNO<sub>3</sub> stock solution, 5.0 ml of biological buffer solution (MES for pH values of 5.15 and 6.1; CHES for pH values of 9.3; HEPES for pH values of 7.5) and required amount of 1.487M NaOH in a 50 ml volumetric flask. (iii) The flask was filled with deionized water upto the 50ml mark. This way by changing the amount of arsenic stock solution, the arsenic concentration was varied from 0.1ppm to 25.0ppm and by changing the amount of NaOH the pH was kept constant at values of 5.15, 6.1, 7.5 and 9.3. (iv) The prepared aqueous solution was taken in a 50ml centrifuge tube and 0.005g HNP was added in the solution; the resulting HNP concentration was 0.1g/L. (v) At the beginning of each experiment the HNPs were dispersed in solution by sonication using a sonication probe (Sonifier(R), Branson Sonic Power Company Danbury, Connecticut, Power Supply, B-12.) for 10 min. (vi) The hematite nanoparticle suspension in the centrifuge tubes was equilibrated in an end-over-end rotator (Fig.: 4.2) for 24 hours at a constant speed of 20rpm. (vii) After 24 hours the supernatant from the 50ml centrifuge tubes were taken into 15 ml centrifuge tubes, and the 15ml tubes were centrifuged for 10 minutes to settle the HNP in the bottom portion of the tube. (viii) The supernatant solutions were filtered through 0.2 μm Nalgene syringe filters (Surfactant Free Cellulose Acetate, SFCA). (ix) The pH was measured immediately after filtration. (viii) Arsenic concentration of the clear liquid collected from the tubes was measured after suitably diluting the sample.

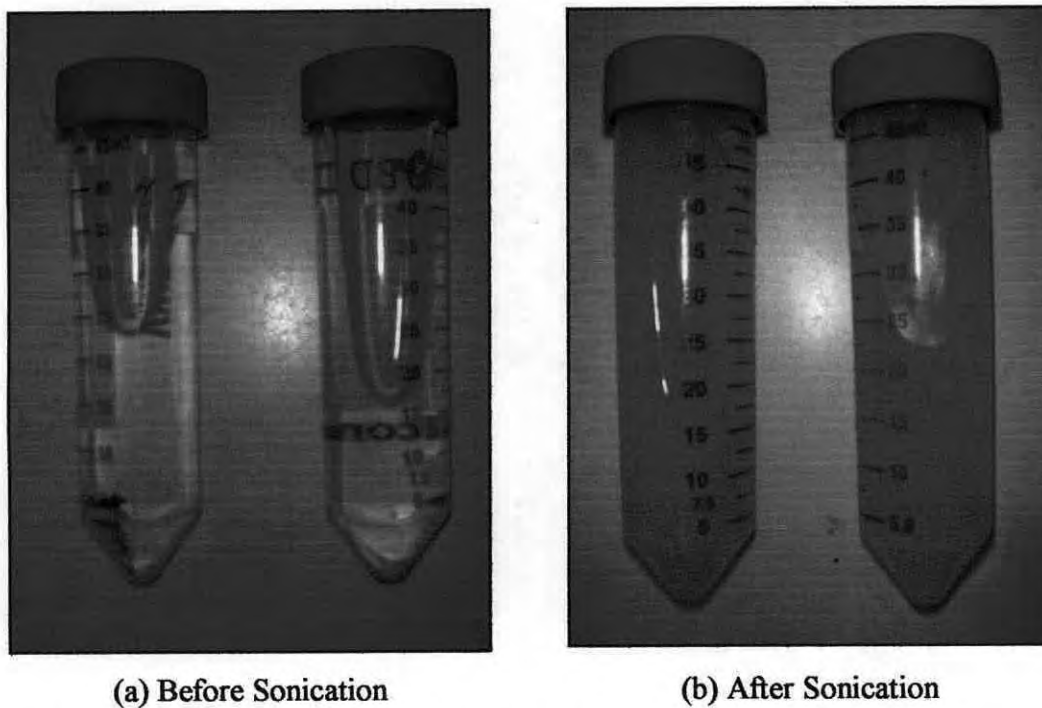


**Figure 4.1:** Effect of Sonication on dispersion of Hematite Nanoparticles

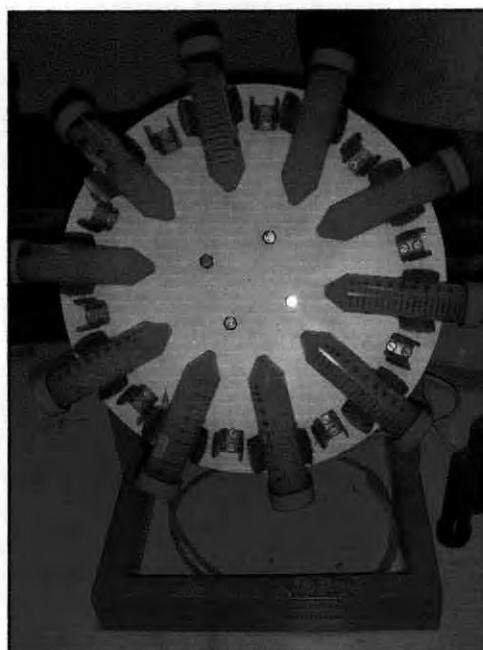


**Figure 4.2:** Equilibration of the hematite suspension in an end-over-end rotator

(ix) The amount of adsorbed arsenic was estimated by using the initial and final concentrations of arsenic in the aqueous solutions.



#### Adsorption of Arsenic present in Natural Groundwater:

Adsorption of arsenic from groundwater was analyzed in batch adsorption tests similar to those described above. The only difference is in step (iii) where BUET groundwater was used instead of deionized water to prepare a solution with arsenic concentration of 1.0 ppm. No buffer was used to control the pH, and the tests were conducted at natural pH. The hematite nanoparticles concentration was maintained at 0.1 g/L.

#### *Effect of Dispersion of Hematite Nanoparticles on Adsorption of Arsenic*

In order to assess the effect of dispersion of hematite nanoparticles on adsorption of arsenic another set of batch experiment was performed in addition to the usual batch experiments mentioned in the previous article. In this case the experimental protocol followed was similar to that mentioned in the previous article, except no sonication was done to disperse the HNPs as mentioned in step (v). Instead the 50ml centrifuge tubes were sealed tightly and manually shaken for 1min before it was equilibrated in the end-over-end tumbler for 24 hours at 20 rpm. Only arsenite, As(III) solutions was used to detect the effect of dispersion of hematite nanoparticles on the adsorption of arsenic.

#### *Effect of pH on Adsorption of Arsenic*

Effect of pH on adsorption of arsenic on HNP was assessed by batch adsorption experiments similar to those described in previous article, except no biological buffer was used in step (ii). After filling the glass volumetric flasks to 50ml mark with deionized water, the pH of the solution was varied by adding dilute hydrochloric acid (0.5M) or sodium hydroxide (0.5M) in amounts of several micro liters. In these adsorption experiments the arsenic concentration was kept constant at 1.0 ppm. The dilute acid and base solutions were used to achieve a wide range of pH (pH = 3~10).

#### *Adsorption of Phosphate*

Arrangements of the batch adsorption tests for phosphate were similar as that discussed in the previous article. The only difference is that instead of arsenic,

standard stock solution of phosphate (10 ppm) was used to prepare the aqueous solution. The initial phosphate concentration was taken to be 0.1 ppm, 0.5 ppm and 1.0 ppm. The pH of the solution was kept constant at 6.1 using 5.0ml of 0.5 M MES buffer and 0.75ml of 1.487 M NaOH. The concentration of hematite nanoparticles was 0.1 g/L. Phosphate concentration was determined using a spectrophotometer (Hach, DR4000U). The difference between the initial and residual phosphate concentration gave the quantity of adsorbed phosphate on hematite nanoparticles.

#### *Effect of Phosphate on Arsenic Adsorption*

Effect of phosphate concentration on adsorption of arsenic on HNP was assessed in similar batch experiments described in the previous article. In these experiments HNP concentration was 0.1 g/L, arsenic (both arsenite and arsenate) concentration was fixed at 0.5 ppm, while phosphate concentration was varied from 0.10 ppm to 0.50 ppm. The concentration of phosphate was varied by adding required amount of phosphate stock solution of 10ppm in step (ii). In all experiments, pH was also kept constant at 6.1 (using 5.0ml of 0.5 M MES buffer and 0.75ml of 1.487 M NaOH). Residual phosphate concentration was determined using a spectrophotometer (Hach, DR4000U), while arsenic concentration was determined using AAS attached with a graphite furnace (GF-AAS). The difference between the initial and residual phosphate and arsenic concentrations gave the quantity of adsorbed phosphate and arsenic respectively on hematite nanoparticles.

#### 4.2.2 Kinetics of Arsenic adsorption on Hematite Nanoparticles

Batch experiments were performed to evaluate the kinetics of adsorption of arsenic on HNPs. The rate of arsenic adsorption is an important factor for arsenic removal. For this experiment, 5ml of arsenic (arsenite or arsenate) stock solution of 100 ppm was added in a 500-ml glass volumetric flask, along with 50ml of 0.5 M MES, 5ml of 0.1M NaNO<sub>3</sub> and 8.5ml of 1.487M NaOH. The volumetric flask was then filled to the 500ml mark with distilled water. Finally the 500ml solution was taken in a glass beaker. The initial arsenic concentration of the solution was 1.0 ppm with a background electrolyte concentration of 0.01M NaNO<sub>3</sub>. The pH of the solution was

fixed at 6.1. The solution was constantly stirred with a magnetic stirrer. Then 0.05g of HNP was added to the solution (to make the concentration of the HNPs 0.1g/L) followed by 10 minutes of sonication for dispersion of the hematite nanoparticles in the solution. Starting of the reaction time was taken from the time when sonication was stopped. Approximately 10 ml aliquots were taken from the suspension at the following intervals: 0.5, 1.0, 1.5, 2.0, 2.5, 3.0, 3.5, 4.0, 4.5, 5.0, and 22.0, 23.0, 24.0 hours from the start of the reaction time. During this time period a magnetic stirrer was used to agitate the suspension. The collected samples were taken in a 15ml centrifuge tube and centrifuged for 2 minutes to separate the HNP by settling at the bottom of the tubes. The supernatant samples were then filtered through a 0.2  $\mu\text{m}$  Nalgene syringe filter (Surfactant Free Cellulose Acetate, SFCA). Arsenic concentration of the filtrate was measured after suitably diluting the sample. The amount of adsorbed arsenic was estimated by using the initial and final concentrations of arsenic in the aqueous solution.

#### 4.2.3 Laboratory Analysis of Water Samples

Water from the acidified samples was used in the laboratory for analysis of total As and Fe. Water from the non-acidified samples collected after filtration was used for analysis of other water quality parameters, including pH, phosphate.

Arsenic concentrations were determined with an AAS (Shimadzu, Japan, AA6800) attached with a graphite furnace. Iron concentrations were determined with flame emission atomic absorption spectrophotometry, using an AAS (Shimadzu, Japan, AA6800). Detection limits of arsenic and iron were  $1\mu\text{g/L}$  and  $0.02\text{ mg/L}$ , respectively. pH was determined using a pH meter (HACH Co., USA) and phosphate concentration was determined with a spectrophotometer (HACH Co. USA, DR4000U). Phosphate was measured by the Molybdenum Blue method and the detection limit was  $0.01\text{ mg/L}$ .

Standard QA/QC protocol was followed throughout, including replicate analysis (1 in every 5 samples), checking of method blanks (1 in every 10 analysis) and standards (1 in every 10 analysis).

#### 4.2.4. Chemicals and Reagents used

All chemicals used in this study were of analytical grade. Deionized water from a Barnstead Fistream III Glass Still distiller was used throughout. Stock solutions of arsenic ( $1000 \pm 10$  mg/L as  $\text{As}^{3+}$ , prepared from  $\text{As}_2\text{O}_3$ ; May & Baker Ltd., Dagenham, England and  $1000 \pm 10$  mg/L as  $\text{As}^{5+}$ , prepared from  $\text{Na}_2\text{HAsO}_4 \cdot 7\text{H}_2\text{O}$ ; MERCK, E. Merck, Darmstadt) were used for preparation of standard solutions for AAS. Arsenic standard solutions of 10, 20, 30, 40  $\mu\text{g/L}$  were prepared for GF-AAS analysis. Iron standard solutions of 1, 2, 3 and 4 mg/L were prepared for Flame-AAS analysis. Standard solutions were prepared daily and the calibrations curves for arsenic and iron were also prepared daily using standard solutions. Stock solution of phosphate ( $100 \pm 1.0$  mg/L as  $\text{PO}_4$ , HACH Co., USA) was used for preparation of standard solutions for measurement of phosphate concentrations using a spectrophotometer (HACH Co., USA). Hematite Nanoparticles were procured from Nanostructured and Amorphous Materials, Inc. (16840 Clay Road, Suite 113 Houston, TX 77084, USA).

All acids used in this study were of analytical grade. Hydrochloric acid (fuming 37%, extra pure, Merck, Germany), Nitric acid (65%, extra pure, Merck Germany) and Sulfuric acid (95-98%, extra pure, Merck, Germany) were used throughout.

### 4.3 Results And Discussion

#### 4.3.1 Effect of pH on Arsenic Adsorption

Effect of pH on adsorption of arsenite and arsenate on HNPs was assessed in batch experiments. It may be noted that in all experiments the initial arsenic concentration

of the solution was 1.0 ppm (0.133 mol As / kg HNP) and the HNP concentration was 0.1 g/L.

Figure 4.3 shows a plot of final pH of water versus the quantity of Arsenic adsorbed on hematite (expressed as mol/kg). Effect of pH on adsorption of both arsenite and arsenate appear to follow the same trend. Adsorption of arsenite was more than that of arsenate for  $\text{pH} > 5.0$ . For  $\text{pH} < 5.0$  the adsorption of arsenite and arsenate were almost similar.

With increasing pH there was an initial decrease of arsenate adsorption onto hematite nanoparticles with the maximum adsorption of 0.065 mol/kg occurring at around pH 4.0 and minimum adsorption of 0.040 mol/kg at around pH 7.0. After that the adsorption of arsenate increased gradually to about 0.058 mol/kg at around pH 10.0. However, the adsorption values in the lower pH range ( $\text{pH} = 2\sim 4$ ) was more than that in the higher pH range ( $\text{pH} > 9.0$ )

Similar but less pronounced trend was observed for the adsorption of arsenite on hematite nanoparticles. The maximum adsorption of hematite nanoparticles was around 0.070 mol/kg of hematite, observed at both the lower pH (around pH 3.5) and higher pH (around pH 9.0), with the minimum adsorption of 0.055 mol/kg occurring at around pH 6.0.

The decrease in adsorption of arsenate and arsenite in the pH range of 5.0~7.5 can be attributed to the aggregation characteristics of the hematite nanoparticles which is related to the surface charge characteristics of HNP (discussed in Section 3.3.4). As discussed in the next Section (4.3.2), aggregation has a significant influence on arsenic adsorption on HNPs. In the pH range from 3.0 to 7.0 the surface charge of the hematite nanoparticle is positive. With increasing pH the surface charge changes gradually to zero at  $\text{pH} = 6.0\sim 7.0$ . After that the surface charge becomes negative at higher pH values. The pH effect on aggregation is mainly due to the fact that pH affects particle surface charge. As pH increases, the ionization of surface function group increases, and positive charge on particle surface decreases. This indicates that

the surface area property dominates the adsorption characteristics more in this pH range.

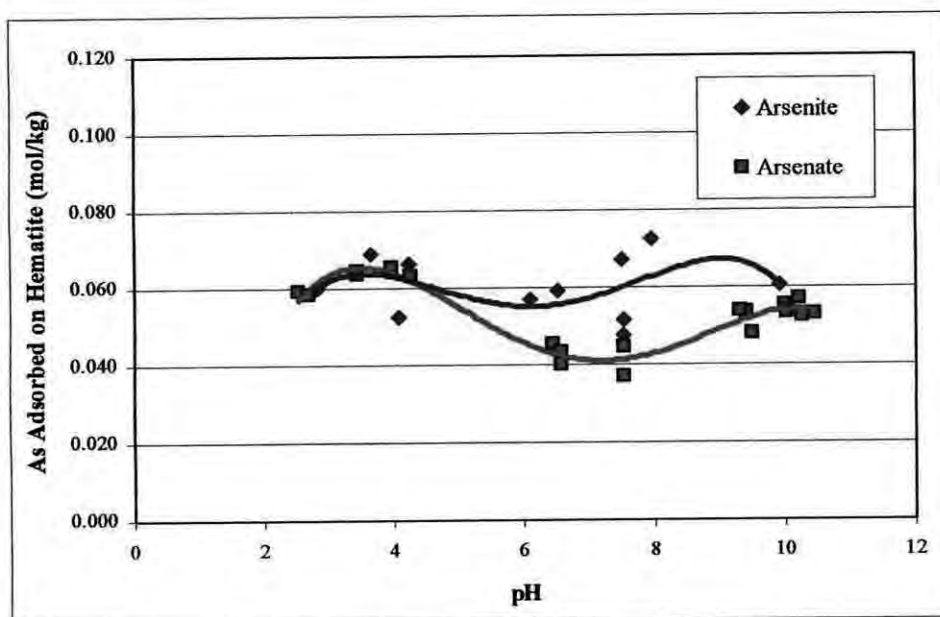


**Figure 4.3:** Adsorption envelopes of As(III) and As (V) with Hematite NP at 0.1 M ionic strength. (0.133 mol As / kg Hematite)

In the low pH region, where the particles retain sufficient positive charge, the nanoparticles are stabilized due to electrostatic repulsion. As pH increases, surface group deprotonation increases and will finally reverse the charge into negative. During this change, the degree of destabilization will be a maximum due to charge neutralization (He et al. 2005). Thus aggregation of hematite nanoparticles is likely to occur around the  $pH_{pzc}$  value, that is pH 6.5 (see Section 3.3.4), which may cause the available adsorption sites to decrease causing less adsorption of arsenic.

Also the predominant oxidation state of arsenate in low pH range (pH 3~6) is  $H_2AsO_4^-$  and it causes more adsorption of arsenate on hematite nanoparticles as the nanoparticle surface is positively charged. On the other hand at high pH range (pH 7~11), the predominant oxidative state of arsenate is  $HAsO_4^{2-}$ . Hence the adsorption on hematite nanoparticle surface is less at high pH since the surface is negatively charged. So apart from the mid region of pH values where aggregation of hematite nanoparticles occurs causing decrease in adsorption, there is a general lowering of adsorption of arsenate as pH increases.

In case of As (III) species, the un-dissociated  $H_3AsO_3$  predominates at pH values less than 9.2. Hence the adsorption of arsenic is not significantly affected by the surface charge of the nanoparticle, and it is reduced only in the mid region of pH (around pH 6.5) because of decreased surface area due to aggregation, when surface charge approaches neutral value.

#### 4.3.2. Effect of Dispersion of Hematite Nanoparticles on Arsenic Adsorption

Table 4.1 shows the effect of dispersion of hematite nanoparticles on adsorption of arsenite. The aggregation of hematite nanoparticles was one of the important issues related to hematite application for arsenic removal. In our study, sonication was used to break hematite nanoparticles aggregates. Table 4.1 shows that when sonication was used arsenic adsorption on HNPs increased significantly. The use of sonication is indicative of the significance of de-aggregation of nanoparticles.

**Table 4.1:** Effect of hematite aggregation on adsorption of arsenite, As(III)

Initial Concentration of As(III), ppb	As (III) Adsorbed, ppb (without sonication)	As (III) Adsorbed, ppb (with sonication)	% increase in adsorption due to sonication
100	86.3	95.7	10.9
500	252.5	304.5	20.6
1000	343.9	433.2	26.0
10000	457.5	917.9	100.7
20000	920.8	3553	285.9
25000	540.7	2533	368.5

It can be seen that sonication caused the dispersion of hematite nanoparticles resulting in smaller particles with increased surface area for adsorption. These resulted in significant increase in the adsorption capacity of hematite nanoparticles; by about 10% for lower concentration of arsenite and by about 370% for higher concentration of arsenite. Hence it is evident that the extent of aggregation of hematite nanoparticles can substantially affect its adsorption capacity.

### 4.3.3 Adsorption of Arsenic on Hematite Nanoparticles

The adsorption characteristic of arsenic was assessed from adsorption isotherms. The adsorption capacities of the hematite nanoparticles for As(III) and As(V) were evaluated using the isotherms presented in Fig. 4.4 and 4.5, respectively.

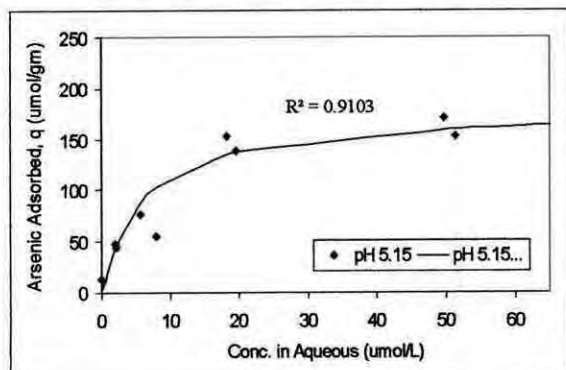
The Langmuir and Freundlich equations were employed to describe the adsorption isotherms in the figures. The maximum adsorption calculated from the Langmuir equation was used as the arsenic adsorption capacity. The adsorption constants obtained from the isotherms at different experimental conditions are listed in Table 4.2. As shown in Table 4.2, relatively high regression coefficients ( $R^2$ ) suggest that both Langmuir and Freundlich models are suitable for describing the adsorption behavior of arsenic by hematite nanoparticles.

**Table 4.2:** Langmuir and Freundlich isotherm parameters for As(V) and As(III) adsorption on Hematite Nanoparticles.

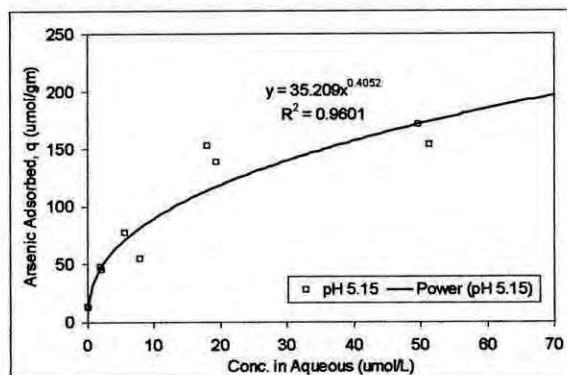
pH	As Species	Langmuir model			Freundlich model		
		$q_m$ ( $\mu\text{mol/g}$ )	B ( $\text{L}/\mu\text{mol}$ )	$R^2$	$K_F$ ( $\text{L}/\mu\text{mol}$ )	n	$R^2$
5.15		180	0.170	0.9103	31.68	4.29	0.9601
6.1	As (III)	590	0.030	0.9217	24.03	1.55	0.9192
7.5		590	0.030	0.9403	36.02	1.85	0.9083
5.15		170	0.335	0.9110	39.40	2.43	0.8738
6.1	As (V)	300	0.135	0.9274	41.35	1.99	0.9790
9.3		435	0.016	0.9614	7.49	1.13	0.9404

The adsorption data presented in Table 4.2 shows that maximum arsenite As(III) adsorption capacity, ( $q_m$ ) of 590  $\mu\text{mol/g}$ . Also the maximum arsenate As(V) adsorption capacity was found to be 435  $\mu\text{mol/g}$ . It is observed that at a given pH value (used in experiments) the affinity for arsenite adsorption is more than that of arsenate.

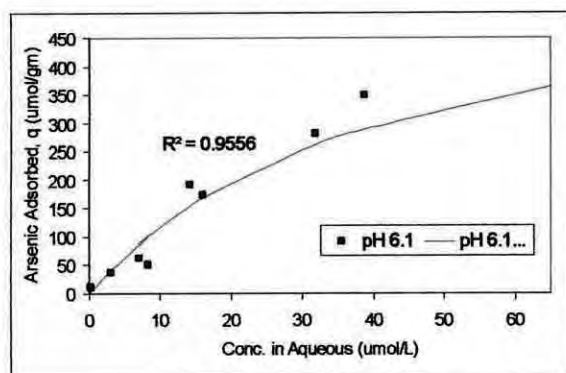


**Langmuir Adsorption Isotherm**

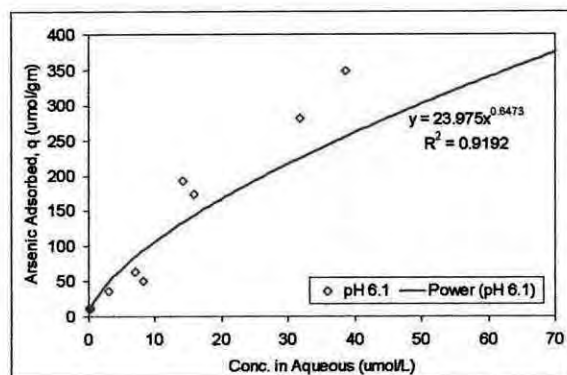
(a)

**Freundlich Adsorption Isotherm**

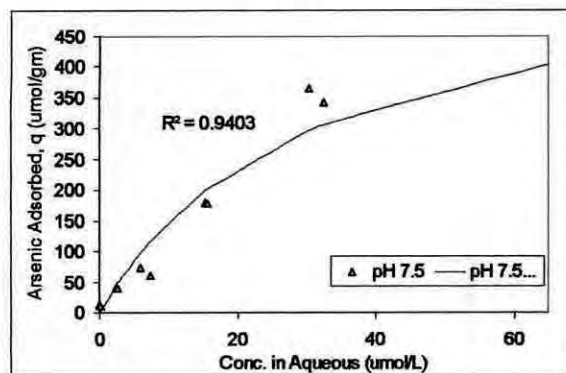
(d)



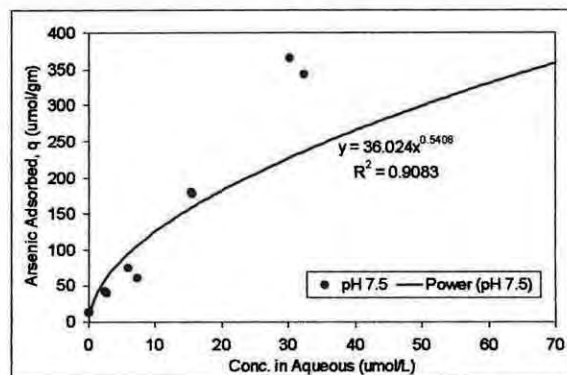
(b)



(e)

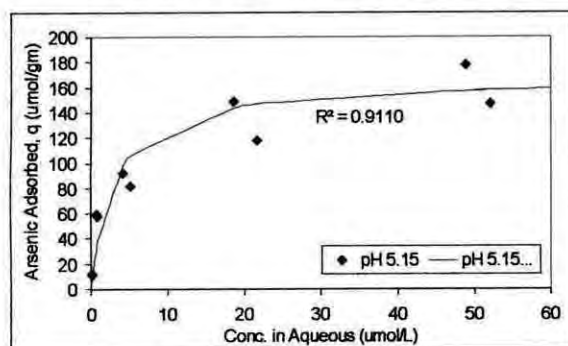


(c)

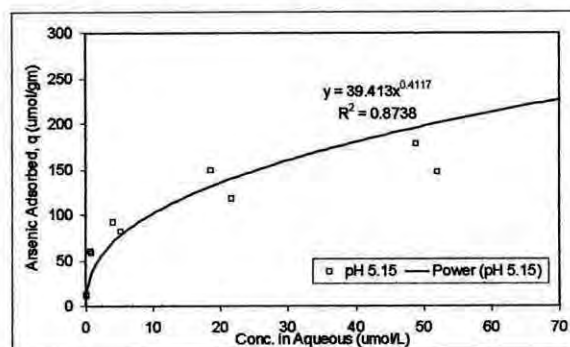


(f)

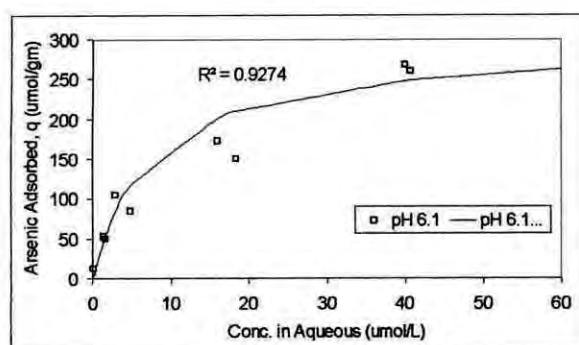
**Figure 4.4:** Adsorption isotherms for As(III) on hematite nanoparticles in a 0.1 g/L suspension at pH 5.15, 6.1 and 7.5.

**Langmuir Adsorption Isotherm**

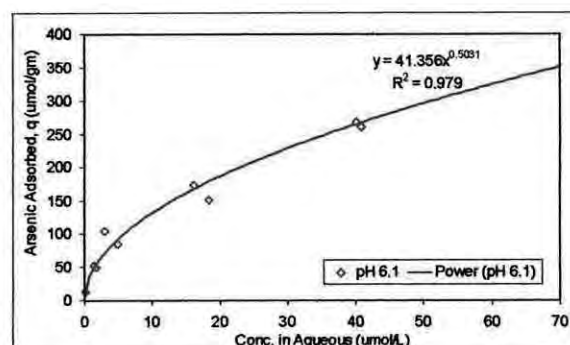
(a)

**Freundlich Adsorption Isotherm**

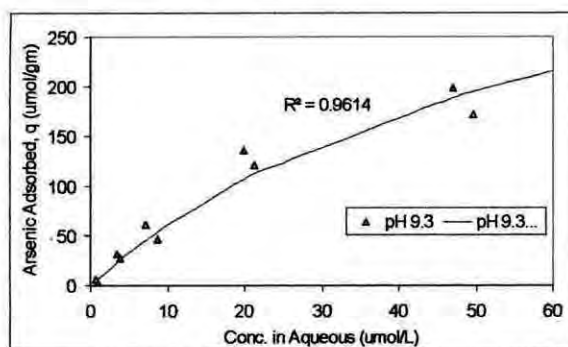
(d)



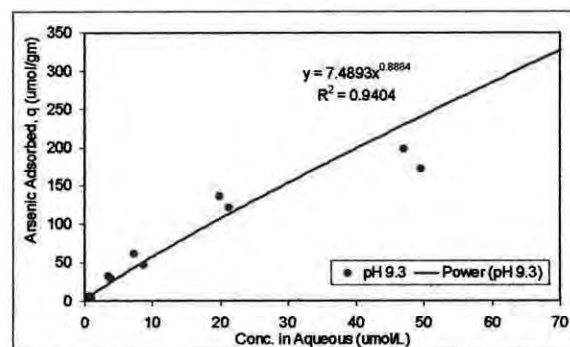
(b)



(e)



(c)



(f)

**Figure 4.5:** Adsorption isotherms on As(V) by hematite nanoparticles in a 0.1 g/L suspension at pH 5.15, 6.1 and 9.3.

Here the observed Langmuir and Freundlich Isotherms denote certain characteristics of adsorption of arsenic on HNPs. The Langmuir isotherm appears to form a plateau with increasing concentration of arsenic which indicates the completion of the mono-

layer coverage of the sorbent. It must be noted that Langmuir isotherm explains mono-layer adsorption phenomenon. On the other hand no such plateau is visible in the Freundlich Isotherms as it shows increase in adsorption of the sorbate onto the sorbent with increasing concentration of sorbate. The Freundlich isotherm is suitable to describe multi-layer adsorption, i.e. after completion of the surface coverage adsorption continues on initial layers of adsorbed sorbate material, so instead of a plateau a gradual increase in the adsorbed quantity is shown in the Freundlich isotherms.

The obtained  $q_m$  values obtained for the hematite nanoparticles are compared with those obtained using other adsorbents in Table 4.3.

Adsorbent	Max. As(III)	Max. As(V)	Reference
	Adsorption capacity (mmol g <sup>-1</sup> )	Adsorption capacity (mmol g <sup>-1</sup> )	
<b>Hematite Nanoparticles</b>	<b>0.59 (pH 6.1)</b>	<b>0.30 (pH 6.1)</b>	<b>Present study</b>
MnO <sub>2</sub>	0.13	0.1	Lenoble et al. (2004)
Goethite	/	0.53 (pH 3-3.3)	Matis et al. (1997)
Al <sub>2</sub> O <sub>3</sub> /Fe(OH) <sub>3</sub>	0.12 (pH 6.1)	0.49 (pH 7.2)	Hlavay and Polyák (2005)
Fe(III)-loaded sponge	0.24 (pH 6.1)	1.83 (pH 4.5)	Muñoz et al. (2002)
Fe-Mn-mineral material	0.16 (pH 6.1)	0.09 (pH 5.5)	Deschamps et al. (2005)
TiO <sub>2</sub>	0.43 (pH 6.1)	0.55 (pH 7.0)	Bang et al. (2005)

Most of the traditional media used for arsenic removal have very low selectivity for arsenite. It should be noted that majority of arsenic in natural groundwater exists as arsenite (WHO, 2005). Hence the increased maximum adsorption capacity for arsenite holds great potential for the use of hematite nanoparticles as an effective adsorbent for arsenic removal, without the necessity of using an oxidizing agent for converting arsenite to arsenate.

### Review on Arsenite and Arsenate Adsorption on Hematite Nanoparticles:

The adsorption characteristics of arsenic discussed in Section 4.3.3 showed, for HNPs, the maximum adsorption capacity ( $q_{\max}$ ) of arsenite was more than that of arsenate. However, a more in-depth analysis of the adsorption isotherms for both arsenite and arsenate is needed for better understanding of the adsorption phenomenon.

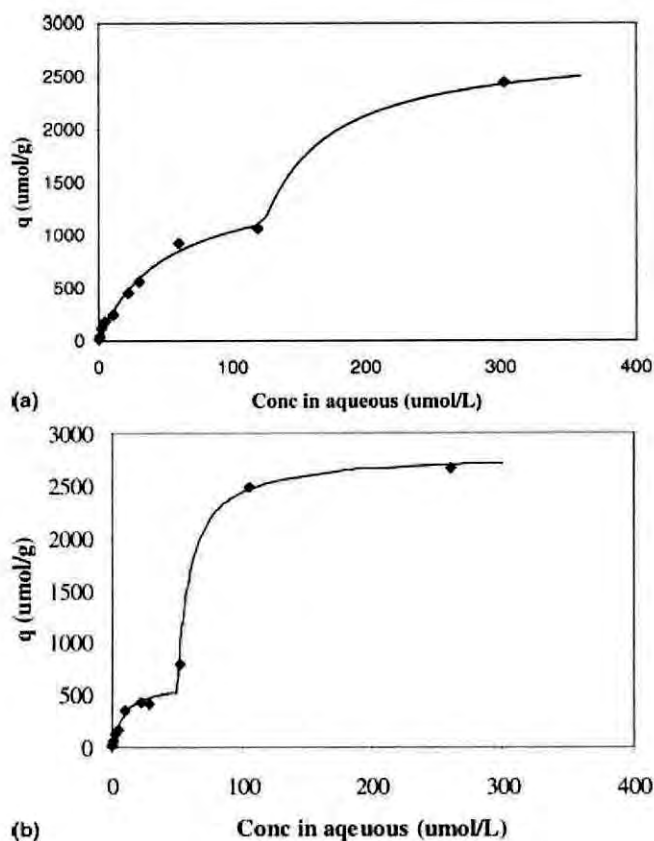
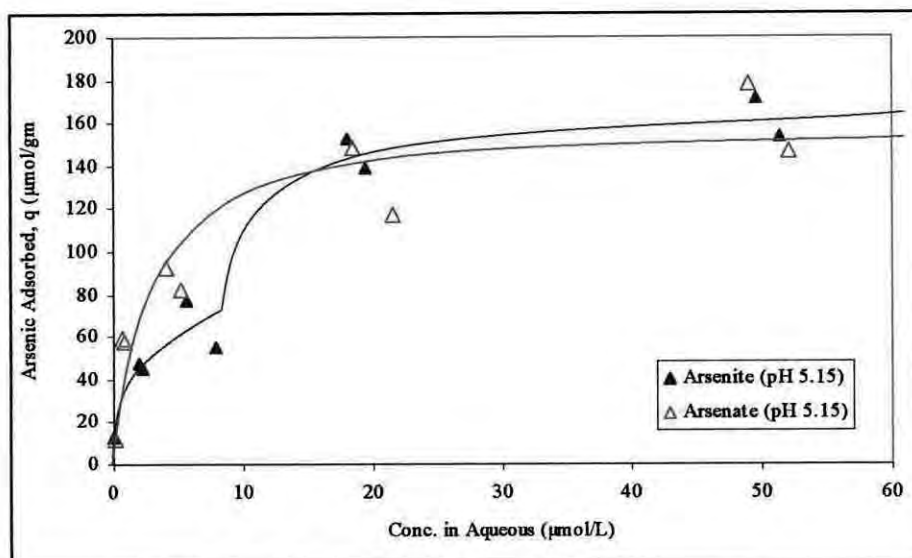


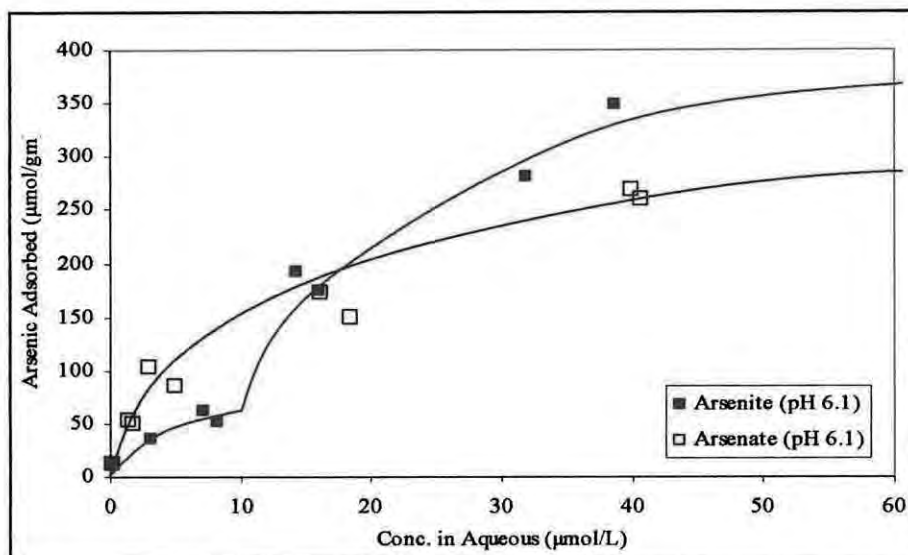
**Figure 4.6:** Adsorption of Arsenic to 11.72 nm magnetite at pH 8.0: (a) As(III) and (b) As(V) (Yean et al., 2005)

Previous works regarding adsorption of arsenic on magnetite nanoparticles (Yean et al., 2005) showed that arsenic adsorption isotherm appeared to consist of two Langmuir type isotherms for both arsenite and arsenate. Figure 4.6 shows the adsorption isotherms for As(III) and As(V) on magnetite nanoparticles (size: 11.72

nm) reported by Yean. It shows that at low concentration, the adsorption isotherms can be fitted with a simple Langmuir Isotherm. However, at high As concentrations, the adsorption data deviates from the simple Langmuir isotherm, and appears to follow a second Langmuir isotherm.



(a)



(b)

**Figure 4.7:** Adsorption of Arsenite and Arsenate on HNPs: (a) pH 5.15, (b) pH 6.10. A closer look at the adsorption data generated in the present study revealed a similar trend for adsorption of arsenite. It was found that arsenite adsorption plots consisted

of two Langmuir type isotherms as discussed above, and in case of arsenate only one Langmuir type isotherm was sufficient to describe the experimental data. The adsorption isotherms are shown in Figure 4.7.

From Figure 4.7 it is seen that at low concentration range ( $<17 \mu\text{mol/L}$ ) of arsenic the adsorption of arsenate was more than that of arsenite. However, for arsenic concentrations greater than  $17 \mu\text{mol/L}$ , adsorption of arsenite was gradually increasing and became higher than that of arsenate. Figure 4.7 shows arsenic adsorption plots for pH values of 5.15 and 6.10. From these adsorption isotherms, the calculated maximum adsorption capacity of arsenite and arsenate were similar to those reported in Table 4.3.

These characteristics are very important in terms of understanding the adsorption phenomenon properly. Although the maximum arsenite adsorption capacity of HNP is more than that of arsenate, in low range of arsenic concentration the adsorption of arsenate appear to be higher than arsenite. This finding is important to corroborate the kinetics data discussed in Section 4.3.6. A more investigative analysis should be made in the concentration range near  $17 \mu\text{mol/L}$  to obtain more adsorption data and determine the true shape of the adsorption isotherm.

#### *Adsorption of Arsenic from Ground Water*

The adsorption of arsenic from BUET ground water was evaluated at natural pH (pH 7.5) of the groundwater, with a hematite nanoparticles concentration of  $0.1 \text{ g/L}$ . The groundwater was collected from a deep tube-well adjacent to the Administrative Building of BUET and results of adsorption of arsenic on nanoparticles are shown in Table 4.4. Table 4.4 shows that adsorption of both As(III) and As(V) are comparable.

Quantities of As adsorbed, presented in Table 4.4, are less than those achieved during laboratory batch experiments (under similar conditions), which were conducted using only aqueous solutions of arsenic.

Arsenic Species	Residual Arsenic Concentration, ppb ( $\text{mmol g}^{-1}$ )	Adsorbed Arsenic, ppb ( $\text{mmol g}^{-1}$ )	% of Arsenic adsorbed
As(III)	597 (0.079)	403 (0.054)	40.3
As(V)	549 (0.073)	451 (0.060)	45.1

Previous research (Sharma, 2006 and Zhang et al., 2007) has shown that arsenic sorption to mineral surfaces decreases in the presence of competing anions such as phosphate, silicate, sulfate, nitrate, carbonate as well as natural organic matter (NOM). Hence the presence of such competing anions in the groundwater may be responsible for the observed lower adsorption of arsenic from natural groundwater. Also the pH value of 7.5 indicates that the surface of the HNPs was negatively charged. Another important reason for lower adsorption could be aggregation of the nanoparticles in the presence of cations such as  $\text{Ca}^{2+}$  and  $\text{Mg}^{2+}$ , which would promote “double layer compression”, resulting in possible increased aggregation.

#### 4.3.4 Adsorption of Phosphate on Hematite Nanoparticles

The adsorption of phosphate on hematite nanoparticles was evaluated at a constant pH of 6.1 and at a hematite concentration of 0.1 g/L. The phosphate adsorption results are shown in Table 4.5. It is seen that with increasing phosphate concentration the percentage removed from the solution increased, and around 60 to 70 percent of the phosphate in the solution was removed by adsorption onto hematite nanoparticles for initial phosphate concentration greater than 0.5 ppm.

Initial Phosphate Concentration. (ppm)	Residual Phosphate Concentration (ppm)	Adsorbed Phosphate. (ppm)	% of Phosphate Adsorbed
0.1	0.086	0.014	14.0
0.5	0.154	0.346	69.2
1	0.388	0.612	61.2

#### 4.3.5 Effect of Phosphate on Adsorption of Arsenic

Among the anions which could compete effectively with arsenic for adsorption site on a sorbent, Phosphate is ubiquitous in natural groundwaters. Groundwater in Bangladesh also contains fairly high concentrations of phosphate (0.2-3.0 mg/L) (Meng et al., 2000). So its potential influences on arsenic sorption and mobility are great. Phosphate sorbs strongly onto iron oxide minerals and can therefore compete with arsenic for surface sites (Dixit and Hering, 2003). Thus, Phosphate ( $\text{PO}_4^{-3}$ ), whose molecular structures are similar to that of arsenic was selected to assess the effects of co-existing anions on arsenic removal. Figure 4.8 shows adsorption of arsenic on HNP at fixed pH of  $6.15 \pm 0.5$ , in the presence of 3 (three) different  $\text{PO}_4^{-3}$  concentration levels (0.1, 0.25 and 0.5 ppm).

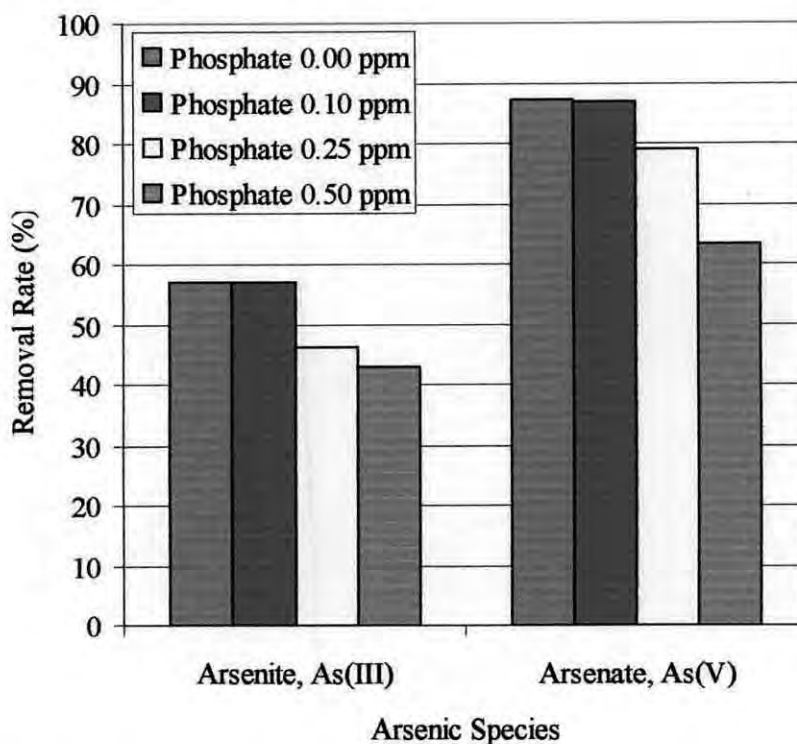


**Figure 4.8:** Effects of co-existing phosphate on arsenite removal at fixed initial arsenic concentration (0.5 ppm) ( $\text{pH } 6.15 \pm 0.5$ , 0.1g/L suspension).

The results presented in Fig. 4.8 shows that arsenic adsorption decreases significantly at relatively high concentration of  $\text{PO}_4^{-3}$ . With a phosphate



concentration of 0.10 ppm the adsorption of arsenic was not affected at all, whereas a phosphate concentration of 0.50 ppm caused the adsorption of arsenite to decrease by about 15% and the adsorption of arsenate to decrease by about 25%.

This high interfering effect of phosphate in the arsenic removal can be explained by the chemical similarity between them. Phosphate element and arsenic element are located in the same main group, and the molecular structure of phosphate ion is very similar to that of arsenic ion. Thus, the present phosphate ion must compete with arsenic ion for adsorptive sites on the surface of hematite nanoparticles.

#### 4.3.6 Kinetics of Arsenic Adsorption on Hematite Nanoparticles

Experiments were performed to determine the rate of arsenic removal from the water by hematite nanoparticles. Fig. 4.9 shows the kinetics of arsenite and arsenate removal and change in concentration of arsenic in the aqueous phase with time. The initial As(III) or As(V) concentration was 13.3  $\mu\text{M/L}$  (1.0 ppm) and the solution pH value was controlled at around 6.1 by adding biological buffer MES and NaOH solution.

The kinetic tests were important to validate the 24hrs equilibration period used in the batch experiments for characterizing arsenic adsorption on HNPs. It was necessary to find out whether the 24hrs time duration was sufficient for the adsorption reaction to reach equilibrium. The kinetic experiment started at 12:00 pm each day and continued for the next five hours upto 5:00 pm. In the next day three samples were withdrawn from the reaction beaker at times 10:00 am, 11:00 am and 12:00 pm. It can be seen from figure 4.9 that after 24 hours, the adsorption of arsenic on hematite nanoparticles reached its equilibrium and the adsorption sites were no longer available for more uptake of arsenic from the solution. In the kinetic test about 83% arsenate and about 47% arsenite were adsorbed in 24 hours. The last three readings of each 24hrs kinetics experiments gave almost equal amount of residual arsenic in the solution.

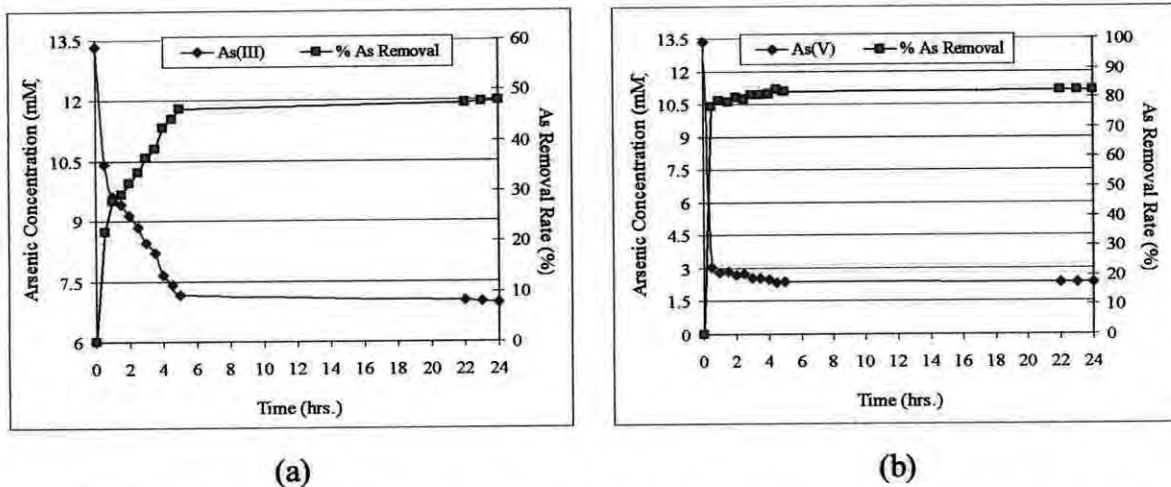


**Figure 4.9:** Kinetics of arsenic [(a) arsenite, As(III); (b) arsenate, As(V)] removal and change in concentration of arsenic species in the aqueous phase with time.

Initial arsenic = 13.3 μM/L; adsorbent content = 0.1 g/L; pH= 6.1.

The kinetic experiment results show that arsenate was more quickly adsorbed onto hematite nanoparticles surface than arsenite. About 80% of arsenate was removed in the first two hours of adsorption reaction. On the other hand about 32% of arsenite was removed in the first couple of hours of adsorption. After 4 and 5 hours, the arsenite removal were 42.5% and 46.5%, respectively.

Kinetic rate constants for the pseudo first order kinetic model and pseudo second order kinetic model were determined from the following two equations (described in article 2.11);

$$\log(q_e - q) = \log q_e - \frac{k_1 t}{2.303} \dots\dots\dots \text{(First-order kinetic model)}$$

$$\frac{t}{q} = \frac{1}{k_2 q_e^2} + \frac{t}{q_e} \dots\dots\dots \text{(Second-order kinetic model)}$$

Figure 4.10 and 4.11 shows the plots of  $\log(q_e - q)$  versus  $t$  and  $t/q$  versus  $t$ , respectively, from which the kinetic rate constants were determined. Table 4.6 lists the computed results obtained from the first-order and the second-order kinetic model and also the experimentally observed values of  $q_e$ .

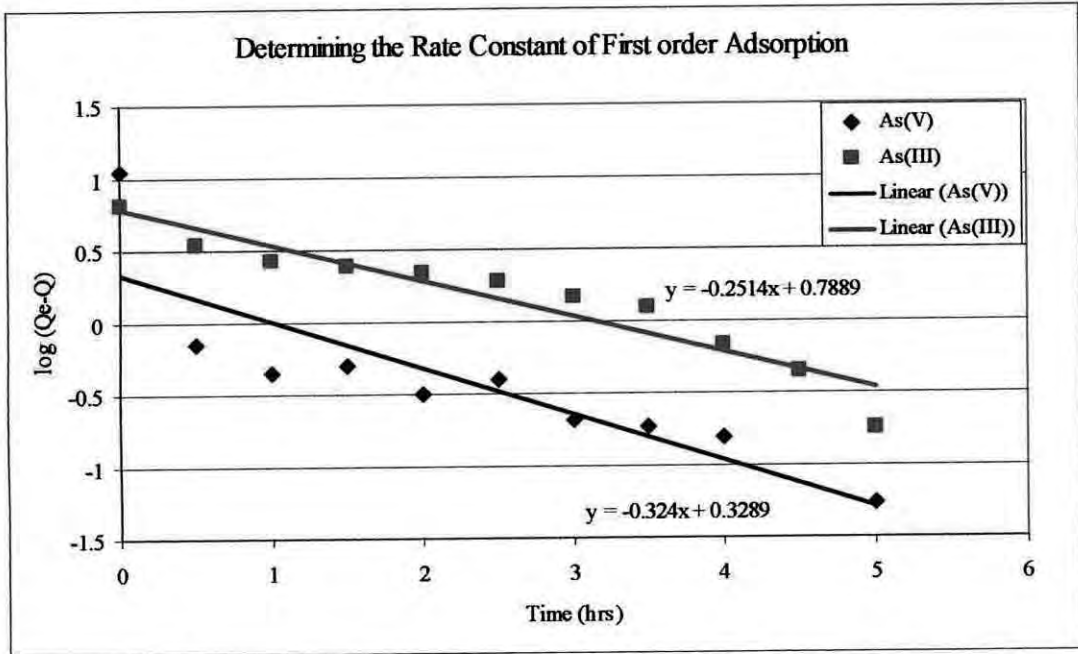


**Figure 4.10:**  $\log(q_e - q)$  versus  $t$ . (Slopes and Intercepts of the graphs were used to determine Reaction Rate Constant  $k_1$ , and amount amount of arsenic adsorbed in equilibrium  $q_e$ )

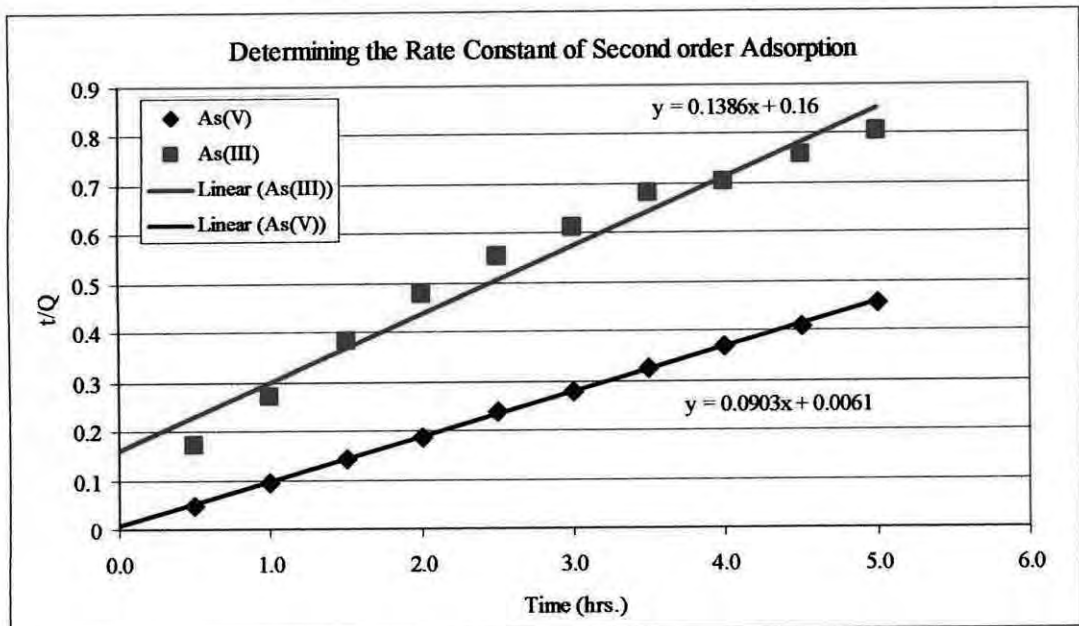


**Figure 4.11:**  $t/q$  versus  $t$ . (Slopes and Intercepts of the graphs were used to determine Reaction Rate Constant  $k_2$ , and amount amount of arsenic adsorbed in equilibrium  $q_e$ )

**Table 4.6:** Comparison of the first-order and second-order adsorption rate constants, and calculated and experimental  $q_e$  values for both As(V) and As(III).

Arsenic	$q_{e,exp}$ ( $\mu\text{M}$ )	First-order kinetic model		Second-order kinetic model	
		$k_1$ ( $\text{hr}^{-1}$ )	$q_{e,cal}$ ( $\mu\text{M}$ )	$k_2$ ( $\mu\text{M}^{-1}\text{hr}^{-1}$ )	$q_{e,cal}$ ( $\mu\text{M}$ )
As (V)	10.93	0.746	2.08	1.337	10.92
As (III)	6.20	0.579	5.81	0.120	5.86

Here we can see that the calculated  $q_e$  values obtained from the first-order kinetic model do not give reasonable value, whereas the calculated  $q_e$  values obtained from the second-order kinetic model agree closely with the experimental  $q_e$  values for all the cases. These suggest that the adsorption of arsenic onto HNPs follows the second-order kinetic model. Also higher value of kinetic rate constant implicates that adsorption of arsenate was faster than that of arsenite.

#### 4.4 Summary

Results from this study show that adsorption of both arsenite and arsenate on hematite nanoparticles vary with the pH of the solution. Effect of pH on adsorption of both arsenate and arsenite appear to follow the same trend. Adsorption of arsenite was higher than that of arsenate. With increasing pH the adsorption decreases to a minimum value at a pH values of around pH 6.0, and then increases again as pH increases. This reduction of adsorption is attributed to the fact that, around pH value of 6.0 the surface charge of the hematite nanoparticles diminishes and the particles aggregate more easily causing a reduction in the effective adsorption surface area. Other than the effect of aggregation at  $\text{pH}=\text{pH}_{\text{pzc}}$ , there is a gradual decrease of adsorption of arsenate from low to high pH. On the other hand, the adsorption of arsenite was more or less same in both the low and high pH ranges.

Langmuir and Freundlich equations were employed to describe the adsorption isotherms. High regression coefficients ( $R^2$ ) suggested that both Langmuir and Freundlich models are suitable for describing the adsorption behavior of arsenic by

hematite nanoparticles. The maximum arsenite As(III) adsorption capacity ( $q_m$ ) was 590  $\mu\text{mol/g}$  at pH 6.1 and the maximum arsenate As(V) adsorption capacity was found to be 435  $\mu\text{mol/g}$  at pH 9.3. This is a very significant finding, which indicates that with high concentration of arsenite, the use of hematite nanoparticles raises the possibility of removing the arsenite from groundwater without the necessity of oxidizing arsenite to arsenate. Hence HNPs can be selected as an efficient adsorbent over most of the traditional media used for arsenic removal having very low selectivity for arsenite. The aggregation of hematite nanoparticles can substantially affect its adsorption capacity. The use of sonication for dispersing the hematite nanoparticles resulted into an increase in the adsorption capacity of hematite nanoparticles by about 10% for lower initial concentration of arsenite and by about 370% for higher initial concentration of arsenite.

It is seen from the test results that with increasing initial phosphate concentration, the percentage removal of phosphate increased reaching around 60 to 70 percent for initial phosphate concentration greater than 0.5 ppm at an HNP concentration of 0.1 g/L. Phosphate is considered as a major anion, which competes with arsenic to take up adsorption sites of hematite nanoparticles. The results of the competitive adsorption between 0.5 ppm arsenic and 0.5 ppm phosphate shows that adsorption of arsenite and arsenate with an initial concentration of 0.5 ppm decreased by about 15% and 25%, respectively, compared to values without the presence of phosphate, in the presence of 0.5 ppm phosphate. Also the use of ground water instead of pure arsenic solution with background electrolyte reduced the arsenic adsorption capacity of hematite nanoparticles, possibly due to the presence of competing anions in natural groundwater.

The kinetic experiments show that the adsorption of arsenic on hematite nanoparticles reached its equilibrium within 24 hours. The results of the kinetic experiment validated the 24 hours equilibration period used in the adsorption experiments.

---

## CONCLUSIONS AND RECOMMENDATIONS

### 5.1 CONCLUSIONS

The present research work commenced with an aim to achieve the following objectives: (1) Characterization of commercially procured hematite nanoparticles, (2) Assessment of arsenic adsorption characteristics of hematite nanoparticles, which included the effect of different water quality parameters like pH, phosphate content along with appraisal of the adsorption kinetics. These informations are needed for developing an arsenic removal system based on hematite nanoparticles.

These objectives were set to understand the adsorption mechanism of arsenic on hematite nanoparticles under different parametric conditions. The conclusions from this study are summarized below:

- Some of the physical qualities of the hematite nanoparticles (e.g. size) mentioned by the manufacturer were different than that observed in the characterization test results. This points out to the essential requirement of characterizing the procured nanomaterials from the commercial vendors, who often do not carry out precise characterization of the materials. It was seen that the reported specific surface area of the nanoparticles  $50 \text{ m}^2/\text{gm}$  was very high compared to the actual specific surface area of  $13.8 \text{ m}^2/\text{gm}$ .
- The pH of zero surface charge ( $\text{pH}_{\text{PZC}}$ ) determined from this study is around 6.5 which is close to the reported value of 7.3 by Plaza et al. Also the XRD analysis showed the composition of the nanoparticles to be  $\alpha\text{-Fe}_2\text{O}_3$  (Hematite) and there was no impurity in the nanomaterials.

- The DLS analysis results showed the size stability of the hematite nanoparticles in suspension. It was observed that at a pH value of 6.1 there was no aggregation of the nanoparticles in the suspension with time. However as the pH value increased and surface charge was gradually diminished, aggregation of the nanoparticles took place and the effective particle size increased with time. At pH 7.5 and pH 6.1 the aggregation rate constants observed were maximum and minimum respectively. It was also observed that even after sonication the effective diameter of the nanoparticles in suspension was more than four times the mean diameter of the nanoparticles observed in the XRD analysis.
- The arsenic adsorption on the sonicated nanoparticles was much higher than those without sonication. This piece of information suggests that adsorption depends on the dispersion of hematite nanoparticles. Hence the effective use of hematite nanoparticles warrants proper dispersion of the nanoparticles in a filter media, or in slurry.
- Adsorption of arsenic on hematite nanoparticles also depends on different water quality parameters like pH, phosphate content. It was observed that with increasing pH the adsorption curve lowers to a minimum value at intermediate pH values (around pH=6.0) and then again increases to a higher value at higher pH. Around pH value of 6.0 (close to the  $pH_{PZC}$  of hematite) the adsorption appears to diminish due to possible aggregation of nanoparticles. Adsorption of dominant arsenite ( $H_3AsO_3$ ) and arsenate ( $H_2AsO_4^-$  and  $HAsO_4^{2-}$ ) appear to be consistent with surface charge characteristics of hematite nanoparticles.
- The results of the competitive adsorption between arsenic and phosphate shows that like other adsorbents, adsorption of arsenic on HNPs decreases in the presence of phosphate ion.

- Kinetics of adsorption shows that the adsorption of arsenic on hematite nanoparticles reaches equilibrium within about 5 hours of contact; adsorption of As(V) was quicker than adsorption of As(III).
- The adsorption isotherm developed from the experimental results shows that both Langmuir and Freundlich isotherm represents the adsorption data well under different parameters. This signifies the fact that multilayer adsorption takes place after initial covering of the adsorbent surface. A closer observation at the adsorption data showed that the data plots for arsenite adsorption consists of two Langmuir type isotherms. This revealed the fact that at lower concentration range of arsenic the adsorption of arsenate was more than that of arsenite. However for higher concentration of arsenic adsorption of arsenite was increasing and eventually became higher than that of arsenate.

## 5.2 RECOMMENDATIONS

The following issues are recommended for future studies to assess hematite nanoparticles as adsorbents for arsenic:

- 1) The desorption characteristics of hematite nanoparticles should be analyzed. This will lead to the assessment of stability of adsorbed arsenic on hematite nanoparticles and of possible regeneration of the hematite nanoparticles used in a filter media.
- 2) Aggregation characteristics of hematite nanoparticles should be studied in more detail (e.g. in the presence of cations/anions) for assuring its potential application in arsenic removal, for example in slurry.
- 3) Studies should be carried out to assess the possibility of impregnating or dispersing the hematite nanoparticles into a porous polymeric matrix, which



will retain the nanoparticles in place and allow them to come in contact with water flowing through the porous material. This way the arsenic present in the water will be adsorbed by the nanomaterials and the entire system can act as an effective filter media.

- 4) Field study should be carried out to see the effect of direct subsurface injection of hematite nanoparticles (e.g., in a slurry), whether under gravity-fed or pressurized conditions to generate a reactive barrier (e.g. around a well), which would act to remove arsenic as contaminated water flows through it. Potential application of the hematite nanoparticles for immobilization of arsenic and other heavy metals should also be studied.

## REFERENCES

- Adachi, Y., Koga, S., Kobayashi, M. and Inada, M. (2005): "Study of colloidal stability of allophane dispersion by dynamic light scattering", *Colloids Surf A* 265:149–154.
- Ahmed, S. A., Sayed, M.H.S.U. and Hadi, S.A. (1998): "Health effects due to Arsenic Toxicity in Bangladesh", Proceedings of the 3rd Forum on Arsenic Contamination of Ground Water in Asia: Effects, Cause and Measures, 22-23 November, Miyazaki University, Japan, p. 59-62.
- Amy, G., Edwards, M., Brandhuber, P., McNeill, L., Benjamin, M., Vagliasindi, F., Carlson, K., and Chwirka, J. (2000): "Arsenic Treatability Options and Evaluation of Residuals Management Issues", Denver, CO: AWWARF.
- Badruzzaman, M., and Westerhoff, P., (2005): "Field and lab-based evaluation of packed bed arsenic treatment systems", AWWA Annual Conference and Exhibition, San Francisco, CA.
- BAMWSP (2005): Bangladesh Arsenic Water Supply Project, Website: [www.bamwsp.org](http://www.bamwsp.org).
- Barrett, E. P., Joyner, L. G. and Halenda, P. P. (1951): "The Determination of Pore Volume and Area Distributions in Porous Substances. I. Computations from Nitrogen Isotherms", *J. Am. Chem. Soc.* 1951, 73, 373-380.
- Begum, S.A. (2001): "Present status and trends in the water supply and sanitation in Bangladesh", M.Engg. Report, Department of Civil Engineering, Bangladesh University of Engineering and Technology (BUET), Dhaka 1000, Bangladesh
- Bentley, R. and Chasteen, T.G., (2002): "Arsenic Curiosa and Humanity", *The Chemical Educator* 7 (2): 51. doi10.1007/s00897020539a
- Berdal, A., Verrié, D. and Zaganianis, E. (2000): "Removal of arsenic from potable water by ion exchange resins", In Greig J.A., Ed., *Ion Exchange at the millennium*. London: Imperial College Press, p. 101.
- BGS/DPHE (2001): Arsenic Contamination of Groundwater in Bangladesh, Department of Public Health Engineering, DFID, British Geological Survey.
- Brunauer, S., Emmett, P. H. and Teller, E. (1938): "Adsorption of Gases in Multimolecular Layers", *J. Am. Chem. Soc.* 1938, 60, 309-319.

- Bulletin of the World Health Organisation (2005): "Arsenic contamination of groundwater and its health impact on residents in a village in West Bengal, India"
- Charles, F. H., Christopher, H. S., Badruzzaman, A. B. M., Keon-Blute, N., Yu, W., Ali, M. A., Jay, J., Beckie, R., Niedan, V., Brabander, D., Oates, P.M., Ashfaque, K.N., Islam, S., Hemond, H.F. and Ahmed, M.F., (2002): "Arsenic Mobility and Groundwater Extraction in Bangladesh", 22, November 2002, Vol 298, *SCIENCE*.
- Chen, A., Wang, L., Battelle, Sorg, T. and Lytle, D. (2004): "Pilot-Scale Evaluation of Adsorptive Media for Arsenic Removal", U.S. EPA, Battelle The Business of Innovation, August 2004.
- Chen, K. L. and Elimelech, M. (2006): "Aggregation and deposition kinetics of fullerene (C-60) nanoparticles", *Langmuir* 2006, 22, 10994-11001.
- Chen, K. L. and Elimelech, M. (2007): "Influence of humic acid on the aggregation kinetics of fullerene (C-60) nanoparticles in monovalent and divalent electrolyte solutions", *J. Colloid Interf. Sci.* 2007, 309, 126-134.
- Chen, K. L.; Mylon, S. E. and Elimelech, M. (2006): "Aggregation kinetics of alginate-coated hematite nanoparticles in monovalent and divalent electrolytes." *Environ. Sci. Technol.* 2006, 40, 1516-1523.
- Coonfare, C.T., Chen, A.S.C., Wang, L., and Valigore, J.M. (2005): "Arsenic removal from drinking water by adsorptive media", USEPA demonstration project at Desert Sands MNWCA, NM. Six month evaluation report. EPA/600/R-05/079.
- Dixit, S. and Hering, J.G. (2003): "Comparison of arsenic (V) and arsenic (III) sorption onto iron oxide minerals: Implications for arsenic mobility", *Environ. Sci. Technol.* 37, 4128 (2003).
- Doušová, B., Grygar, T., Martaus, A., Fuitová, L., Koloušek, D. and Machovic, V., (2006): "Sorption of AsV on aluminosilicates treated with FeII nanoparticles." *Journal of Colloid and Interface Science* 302 (2006) 424-431.
- DPHE/BGS/MML (1999): "Groundwater Studies for Arsenic Contamination in Bangladesh, Final Report (Phase-1), January."
- Driehaus, W., Jekel, M. and Hildebrandt, U. (1998): "Granular ferric hydroxide—A new adsorbent for the removal of arsenic from natural water", *J. Water Serv. Res. Technol.-Aqua*, 47(1), 30.

- EES/DCH (2000): "Groundwater Arsenic Contamination in Bangladesh, A. Summary of Field Survey from August 1995 to February 2000; B. Twenty Seven Days Detailed Field Survey Information from April 1999 to February 2000."
- Elliott, D. and Zhang, W. (2001): "Field assessment of nanoparticles for groundwater treatment", *Environ. Sci. Technol.* 35, 4922–4926.
- Emsley, J. (2001): "Nature's Building Blocks: An A-Z Guide to the Elements", Oxford: Oxford University Press. pp.43,513,529. ISBN 0-19-850341-5.
- USEPA, (2003): "Workshop on Nanotechnology and the Environment." August 28–29, 2002. Arlington, Virginia. P50-51 EPA/600/R-02/080.
- Glazier, R., Venkatakrisnan, R., Gheorghiu, F., Walata, L., Nash, R. and Zhang, W. (2003): "Nanotechnology takes root", *Civil Engineering* 73(5), 64–69.
- He, Y. T., Wan, J. and Tokunaga, T. (2008): "Kinetic stability of hematite nanoparticles: the effect of particle sizes", *J Nanopart Res.* 10:321–332, DOI 10.1007/s11051-007-9255-1.
- Hongshao, Z. and Stanforth, R. (2001): "Competitive Adsorption of Phosphate and Arsenate on Goethite", *Environ. Sci. Technol.*, 2001, 35 (24), pp 4753–4757, **DOI:** 10.1021/es010890y, Publication Date (Web): November 15, 2001, Copyright © 2001 American Chemical Society
- Jain, A., Raven, K. P. and Loeppert, R. H. (1999): "Arsenite and Arsenate Adsorption on Ferrihydrite: Surface Charge Reduction and Net OH<sup>-</sup> Release Stoichiometry", Vol. 33, No. 8, 1999, *Environmental Science & Technology*
- Kanel, S. R., Nepal, D., Manning, B. and Choi, H., (2007): "Transport of surface-modified iron nanoparticle in porous media and application to arsenic(III) remediation", *J Nanopart Res* (2007) 9:725–735. DOI 10.1007/s11051-007-9225-7.
- Kanel, S. R., Manning, B., Charlet, L. and Choi, H., (2005): "Removal of Arsenic(III) from Groundwater by Nanoscale Zero-Valent Iron", Vol. 39, No. 5, 2005, *Environmental Science & Technology*
- Khan, W.A. (1997): "Health effects of arsenic toxicity, WHO Consultation on Arsenic in drinking water and resulting toxicity in India and Bangladesh", WHO New Delhi 29th April – 1st May 1997.
- King, R. J. (2002): "Minerals explained 35: Arsenopyrite". *Geology Today* 18 (2): 72–75. doi:10.1046/j.1365-2451.2002.t01-1-00006.

- Ko, I., Davis, A.P., Kim, J.Y. and Kim, K.W. (2007): "Arsenic Removal by a Colloidal Iron Oxide Coated Sand", *Journal of Environmental Engineering*, Vol. 133, No. 9, September 1, 2007. ©ASCE, ISSN 0733-9372/2007/9-891-898/
- Lagergren, S. (1898): "Handlingar", 24, 1.
- Lee, H. and Choi, W. (2002): "Photocatalytic Oxidation of Arsenite in TiO<sub>2</sub> Suspension: Kinetics and Mechanisms", *Environ. Sci. Technol.*, 2002, 36 (17), pp 3872-3878, DOI: 10.1021/es0158197, Publication Date (Web): August 3, 2002, Copyright © 2002 American Chemical Society
- Manning, B. A., Hunt, M. L., Amrhein, C. and Yarmoff, J. (2002): "Arsenic(III) and Arsenic(V) Reactions with Zerovalent Iron Corrosion Products", Vol. 36, No. 24, 2002. *Environmental Science & Technology*
- Masciangioli, T. and Zhang, W., (2003): "Environmental nanotechnology: Potential and pitfalls", *Environ. Sci. Technol.* 37, 102A-108A.
- Mckay, G., Ho, Y. S. (1999): "Process Biochem.", 34, 451.
- Meng, X., Bang, S. and Korfiatis, G.P. (2000): "Effects of silicate, sulfate and carbonate on arsenic removal by ferric chloride", *Water Res.* 34, 1255.
- North, K.P. (2005): "Attrition loss analysis for arsenic adsorption media", Sandia National Laboratory Report SAND2006-0374.
- Noubactep, C. and Woafu, P., (Manuscript in preparation, 2008): "Elemental Iron (Fe<sup>0</sup>) for Better Drinking Water in Rural Areas of Developing Countries"
- Ouvrard, S., Donato, P.D., Simonnot, M.O., Begin, S., Ghanbaja, J., Alnot, M., Duval, Y.B., Lhote, F., Barres, O. and Sardin, M. (2005): "Natural manganese oxide: Combined analytical approach for solid characterization and arsenic retention"- *Geochimica et Cosmochimica Acta*, Volume 69, Issue 11, 1 June 2005, Pages 2715-2724
- Oxenham, J., Chen, A.S.C. and Wang, L. (2005): "Arsenic removal from drinking water by adsorptive media", EPA demonstration project at Rollinsford, NH. Six month evaluation report. EPA/600/R-05/116.
- Plaza, R.C., Gonzalez-Caballero, F. and Delgado, A.V. (2001): "Electrical surface charge and potential of hematite/yttrium oxide core-shell colloidal particles." *Colloid Polym Sci.* 279:1206-1211 (2001). © Springer-Verlag 2001.

- Puttamraju, P. and Sengupta, A.K. (2006): "Evidence of Tunable On-Off Sorption Behaviors of Metal Oxide Nanoparticles: Role of Ion Exchanger Support, Ind." *Eng. Chem. Res.*, 45, 7737-7742, 2006
- Rubel, F. (2003a): "Removal of arsenic from drinking water by adsorptive media." USEPA Report EPA/600/R-03/019.
- Rubel, F. (2003b): "Removal of arsenic from drinking water by ion exchange." USEPA Report EPA/600/R-03/080.
- Saleh, N. B., Pfefferle, L. D. and Elimelech, M. (2008): "Aggregation Kinetics of Multiwalled Carbon Nanotubes in Aquatic Systems: Measurements and Environmental Implications", *Environ. Sci. Technol.* 2008, 42, 7963-7969.
- Seyferth, D., (2001): "Cadet's Fuming Arsenical Liquid and the Cacodyl Compounds of Bunsen", *Organometallics* 20 (8): 1488-1498. "Digital object identifier" DOI 10.1021/om0101947
- Sharma, P., Kumari, P., Srivastava, S. and Srivastava, M.M., (2006): "Biosorption studies on shelled Moringa oleifera Lamarch seed powder: Removal and recovery of arsenic from aqueous system", *Int. J. Miner. Process.*, 78: 131-139.
- Siegel, M., Aragon, A., Zhao, H., Aragon, M., Everett, R., Nocon, M. and Dwyer, B. (2006): "Determinants of the performance of arsenic adsorbent media: A comparison of field and laboratory studies", Presentation at Spring ACS Meeting, Atlanta, GA, March 2006.
- Sing, K. S. W., Everett, D. H., Haul, R. A. W., Moscou, L., Pierotti, R. A., Rouquerol, J. and Siemieniewska, T. (1985): "Reporting Physisorption Data for Gas/Solid Systems with Special Reference to the Determination of Surface Area and Porosity", *Pure & Appl. Chem.*, Vol. 57, No. 4, pp. 603-619, 1985. Printed in Great Britain. ©1985 IUPAC.
- Sylvester, P., Westerhoff, P., Möller, T., Badruzzaman, M. and Boyd, O. (2007): "A Hybrid Sorbent Utilizing Nanoparticles of Hydrous Iron Oxide for Arsenic Removal from Drinking Water", *ENVIRONMENTAL ENGINEERING SCIENCE*, Volume 24, Number 1, 2007, © Mary Ann Liebert, Inc.
- Turner, A. (1999): "Viewpoint: the story so far: An overview of developments in UK food regulation and associated advisory committees". *British Food Journal* 101 (4): 274-283.
- WHO (1996): "Guidelines for drinking water quality", 2nd ed. Volume 2, p. 158-162.

Yean, S., Cong, L., Yavuz, C.T., Mayo, J.T., Yu, W.W., Kan, A.T., Colvin, V.L. and Tomson, M.B. (2005): "Effect of magnetite particle size on adsorption and desorption of arsenite and arsenate", *J. Mater. Res.*, Vol. 20, No. 12, Dec 2005, © 2005 Materials Research Society

Yu, W., Harvey, C. M. and Harvey, C. F. (2003): "Arsenic in the groundwater in Bangladesh: a geostatistical and epidemiological framework for estimating health effects and evaluating remedies", *Water Resources Research*, 39(6), 2003, 1146

Zhang, G., Qu, J., Liu, H., Liu, R. and Wu, R., (2007): "Preparation and evaluation of a novel Fe-Mn binary oxide adsorbent for effective arsenite removal", *Water Research* 41 (2007) 1921 – 1928

